Supplement: Evaluating Climate Emulation: Fundamental Impulse Testing of Simple Climate Models

Adria K. Schwarber[1], Steven J. Smith[1,2], Corinne A. Hartin[2], Benjamin Aaron Vega-Westhoff[3], Ryan Sriver[3]

[1]Department of Atmospheric and Oceanic Science, University of Maryland, College Park, MD 20742

[2]Joint Global Change Research Institute, 5825 University Research Ct, College Park, MD 20740

[3]Department of Atmospheric Sciences, University of Illinois Urbana-Champaign, Champaign, IL 61820

Correspondence to: Adria K. Schwarber (adria.schwarber@gmail.com)

Contents

S1 Supplementary Method

We conduct perturbations of three contrasting chemical species: carbon dioxide (CO_2), methane (CH_4), and black carbon (BC). We begin with CO_2 because this well-mixed greenhouse gas is the largest contributor to anthropogenic forcing changes (Myhre et al., 2013). Methane is also of interest because it is a shorter-lived greenhouse gas, with chemical interactions with itself and other species (Cicerone, R.J.; Oremland, 1988). Finally, we use BC perturbations to represent aerosols more generally because we are interested in model responses to short-lived climate forcers (Bond et al., 2013; Harmsen et al., 2015). SCM representations of other aerosols species are similar so we do not conduct impulse tests of other species.

The comprehensive SCMs we use are readily comparable because they read in similar emissions. Background trajectory emissions are taken from the published Representative Concentration Pathway (RCP) 4.5 scenario (Thomson et al., 2011) database, which means that all calculations in the main paper are conducted relative to a changing CO_2 concentration background unless otherwise noted. SCMs are often used to project global mean temperature over various future scenarios, so this is the most relevant type of background on which to test these models. Conducting these experiment with a constant CO_2 background, as previously used in the literature (Joos et al., 2013), requires inverse modeling of the individual models to produce constant CO_2 concentration emissions files. Our methodology is easier to implement as a regular unit test as it only requires the same emissions inputs with no inverse calculations needed. We provide the input emission files used in this paper.

In many SCMs, forcing over historical periods is explicitly calibrated to a model base year, so it is not possible to conduct perturbations during these time periods. Therefore, our perturbations are conducted in 2015 to avoid the model base years of our SCMs. In the main paper, we show some model responses out to 2300, the end of the MAGICC model runs, equal to 285 years after the perturbation. Additional results are in S8.

We run reference scenarios in the SCMs, followed by each perturbation case described below. For each experiment (see below) we report the response, which is obtained by subtracting the reference from the perturbation results. For instance, the CO_2 concentration response is obtained as follows:

$$CO_2Concentration_{response}(t) = CO_2Concentration_{perturabtion}(t) - CO_2Concentration_{reference}(t) \quad (1)$$

We conducted the following impulse tests:

a. *Concentration impulse (CO_2).*

These SCMs can be used in a mode where CO_2 concentrations are exogenously specified. We carry out this experiment by instantaneously increasing CO_2 concentration by 200 ppm in 2015. After 2015, CO_2 concentrations return to the baseline levels following the published RCP4.5 scenario. Note, we do not conduct separate forcing impulse experiments because this is functionally equivalent to a concentration impulse. In this experiment, we are only interested in the dynamics of the models' temperature response. This experiment eliminates the added uncertainty in the emissions to concentrations calculation and complicating factors from carbon cycle feedbacks.

b. *Emissions impulse (BC, CH_4, CO_2).*

For this experiment all models were run with an emissions input. We carry out this experiment by increasing individual emissions (BC, CH_4, or CO_2) in one year. Following that year, the emissions return to the RCP4.5 pathway for all subsequent years. In this experiment CO_2 and other GHG concentrations are allowed to vary as determined by each model. We find our perturbation values by doubling the 2015 value for each chemical species equal to a 9.2 PgC pulse of CO_2, a 329 Tg pulse of CH_4, and a 7981 Gg pulse of BC. We also perturb CO_2 emissions in 2010, 2020, 2030, 2040, 2050 to understand changes in model responses over time and see a very small difference in the model response (S4). We compare results from three comprehensive SCMs to two IR models, AR5-IR and FAIR model (Millar et al., 2017; Myhre et al., 2013) (S2).

We also compared results to several ESMs and EMICs by carrying out a 100 GtC CO_2 impulse, following Joos et al. (Joos et al., 2013) (S12). This is approximately 10x the CO_2 perturbation pulse described above.

Finally, we conduct a 4xBC emissions step experiment. We compare the SCM temperature responses with the response of a complex climate model used by Sand et al. (2016) (S13).

c. Step increase in CO_2 concentration (instantaneous 4×CO_2 concentration experiment).
Similar to comparison (a), in this experiment, CO_2 concentrations are prescribed. We have CO_2 concentrations follow a pre-industrial pathway (278.0516 ppmv in 1765) until 2014. The CO_2 concentration is quadrupled (4x) in 2015 and maintained at this level until 2300. This follows the experimental protocol used in the CMIP5 experimental design (Taylor et al., 2012).

We compare these results to drift-corrected (Gupta et al., 2013) global mean temperature results from 20 complex climate models from the CMIP5 archive. We drift-correct the CMIP5 global mean temperature time series by subtracting the slope of the linear fit from the full-time series of the corresponding pre-industrial experiment for each individual model (see S3).

We ran Hector v2.0 with few changes to the default configuration file settings. We changed two model time steps in Hector v2.0: (1) the carbon-cycle-solver.cpp time step from dt(0.3) to dt(0.1) and (2) the ocean_component.hpp OCEAN_MIN_TIMESTEP from 0.3 to 0.01 to allow for the carbon cycle, in particular, the ocean carbon cycle to accurately integrate across the sharp gradient introduced by these experiments. In experiments where we constrained the CO_2 concentration, these changes significantly increase the model run time for this scenario.

Additionally, we used an equilibrium climate sensitivity (ECS) value of 3°C in the SCMs, with the exception of the idealized SCMs, FAIR and AR5-IR (see S2 and Table S10). In both FAIR and AR5-IR, ECS is derived from the choice of ocean parameters given by,

$$ECS = F_{2x}(q_1 + q_2) \tag{2}$$

where F_{2x} is the forcing due to CO_2 doubling ($F_{2x} = 3.74\ Wm^{-2}$) and both q_1 and q_2 are the ocean parameters thermal adjustment of the upper ocean and thermal equilibrium of the deep ocean, respectively (Millar et al. 2017; Equation 4).

We conducted additional sensitivity experiments in the SCMs spanning ranges of climate sensitivity and ocean diffusivity and report the results in S11.

S2 Discussion of Model Specifications

We conduct impulse response tests within three comprehensive SCMs and two idealized SCMs. The three comprehensive SCMs have structural differences worth noting. Hector v2.0, has explicit ocean carbon chemistry in four boxes, where ocean carbon uptake is a non-linear function of the solubility of carbon. MAGICC 5.3 BC-OC and 6.0 have differential hemispheric forcing over land and ocean, thereby calculating temperature over each box. Important characteristics of the carbon and climate components of each model are shown in Table S1.

Table S1 Main carbon cycle and climate characteristics of SCMs and IRFs

Model	Model description	Carbon cycle	Climate component
Hector v2.0 (Hartin et al., 2015, 2016; Kriegler, 2005)	mechanistic climate carbon-cycle model	One-pool atmosphere, three-pool land, and four-pool ocean	Global Energy balance model, with ocean heat diffusion
MAGICC 5.3 BC-OC (Raper and Cubasch, 1996; Smith and Bond, 2014; Wigley and Raper, 1992)	mechanistic climate carbon-cycle model	One-pool atmosphere, three-pool land, and one-pool ocean	4-box Energy balance model, with ocean heat upwelling diffusion
MAGICC 6.0 (Meinshausen et al., 2011)	mechanistic climate-carbon cycle model	One-pool atmosphere, three-pool land, and one-pool ocean	4-box Energy balance model, with ocean heat upwelling diffusion
AR5-IR (Myhre et al., 2013)	Impulse-response function	Impulse-response function	Equilibrium temperature as a function of RF
FAIR v1.0 (Millar et al., 2017)	Impulse-response function	Four timescale impulse-response function with state-dependence of the CO_2 airborne fraction	Equilibrium temperature as a function of RF; IRF with two timescales

Some SCMs also include representations of aerosol dynamics, though the model representations differ. As mentioned in the main paper, unlike Hector v2.0, both versions of MAGICC have differential hemispheric forcing over land and ocean. AR5-IR represents BC forcing response as a simple exponential, similar to the response from greenhouse gas forcing. FAIR v1.0, used here, represents the relationship between CO_2-only emissions, concentrations, and temperature. Other versions of FAIR include non-CO_2 forcing, such as BC.

S2.1 Model Settings

Here we discuss the model settings used in our experiments, noting any changes made to the default settings. All model parameters and input files are provided in the Supplementary Materials.

The three comprehensive SCMs were run with the same ECS values (ECS = 3°C), unless otherwise noted, whereas the ECS in FAIR and AR5-IR depends on the respective model parameters noted in S1 above (see Eq. 2).

We also acknowledge that vertical ocean diffusivity has a large impact on ocean heat uptake and we do note that the SCMs we compare in our paper either do not have the same definitions of vertical ocean diffusivity, as is the case for the comprehensive SCMs, or ocean diffusivity is not directly represented in the models, as is the case for idealized SCMs. For our purposes, therefore, we kept the ocean diffusivity values at their default values within the comprehensive SCMs. Sensitivity experiments exploring the model response to the range of these two parameters derived from MAGICC 6.0 are available in S11.

S2.2 AR5-IR

The IPCC AR5 (Myhre et al. 2013; See caption under Figure 8.28) describes the underlying multi-gas impulse response model used to quantify the multi-gas equivalence metric, Absolute Global Temperature Potential (AGTP), to compare temperature changes at a chosen time in response to a unit pulse of emissions *i*. We refer to this model as AR5-IR and describe below how the sums of exponentials are used to find AGTP and the subsequent temperature response.

AGTP is found via a convolution of the fraction of the species *i* remaining in the atmosphere after an emissions pulse and the climate response to a unit forcing,

$$R_T(t) = \sum_{j=1}^{M} \frac{c_j}{d_j} \exp\left(-\frac{t}{d_j}\right) \text{ (3; See Equation 8.SM.13).}$$

$$AGTP_i(H) = \int_0^H RF_i(t) R_T(H-t) dt \qquad \text{(4; See 8.SM.14)}$$

$$\text{and } RF_i(t) = A_i R_i(t) \text{ (5; See Equation 8.SM.7)}$$

$$\text{where for most species } R_i(t) = \exp\left(-\frac{t}{\tau_i}\right) \text{ (6; See Equation 8.SM.8)}$$

$$\text{and for } CO_2 \; R_{CO_2}(t) = a_0 + \sum_{i=1}^{N} a_i \exp\left(-\frac{t}{\tau_i}\right) \text{ (7; See Equation 8.SM.10)}$$

and A_i is the radiative efficiency yielding, the general equation:

$$AGTP_i(H) = A_i \sum_{j=1}^{2} \frac{\tau c_j}{\tau - d_j} \left(\exp\left(\frac{-H}{\tau}\right) - \exp\left(\frac{-H}{d_j}\right)\right) \qquad \text{(8; See Equation 8.SM.14)}$$

AGTP can then be used to calculate global mean temperature change from any given emission scenario using,

$$\Delta T = \sum \int_o^t E_i(s) AGTP_i(t-s) ds \qquad \text{(9; See Equation 8.1)}$$

where E_i are the emissions of a species, t is the time horizon, and s is the time of emissions (Myhre et al. 2013; See 8.7.13 and Equation 8.1). For this paper, AR5-IR was recoded in R and is available for download with the Supplementaty Materials. Additoinally, a brief discussion of the parameter choices for this model is available in S2.4.

S2.3 FAIR

The FAIR v1.0 model is a modified version of the AR5-IR carbon cycle component to include the state-dependence of the CO_2 airborne fraction to reproduce the relationship between CO_2-only emissions, concentrations, and temperature over the historical period. Millar et al. (2017)

began with the impulse response functions used for calculation of multi-gas equivalence metrics in IPCC-AR5 (Myhre et al., 2013) and extended the CO_2 IRF by coupling the carbon-cycle to the thermal response and to cumulative carbon uptake by terrestrial and marine sinks. FAIR is available for download at https://github.com/OMS-NetZero/FAIR.

FAIR calculates the global mean temperature response as the sum of the temperature response from the fast and slow timescale components, which represent the upper and deep ocean. The model does not report the internally-calculated forcing response, so this is not included in Figure 2 in the main paper.

Here, we use the first iteration of FAIR, but we note that two new versions have recently been published, FAIR v1.1 and FAIR v1.3. FAIR v1.3 extends the original version to, "calculate non-CO_2 greenhouse gas concentrations from emissions, aerosol forcing from aerosol precursor emissions, tropospheric and stratospheric ozone forcing from the emissions of precursors, and forcings from black carbon on snow, stratospheric methane oxidation to water vapour, contrails and land use change (Smith et al., 2018)."

Additoinally, a brief discussion of the parameter choices for this model is available in S2.4.

S2.4 FAIR (without carbon cycle) versus AR5-IR

We expect slight differences in the response of FAIR and AR5-IR to a unit forcing. According to Equation 8 in Millar et al. (2017), FAIR will have a differential response to changing background CO_2 concentrations. By contrast, AR5-IR parameterizes the climate response to a unit forcing, R_T, using a sum of exponentials as given by Equation 8.SM.13 in Myhre et al. (2013):

$$R_T(t) = \sum_j \frac{q_j}{d_j} e^{\frac{-t}{d_j}} \quad \text{(10; See Equation 8.SM.13)}$$

Values of the R_T input parameters, q_j and d_j, are available in Table S2 of this response, where j=1,2 represent the timescales of the fast and slow ocean response. We note all parameters are independent of background concentration in AR5.

In the main paper, we used the time constant parameters representing the thermal equilibrium of the deep ocean (d2) and the thermal adjustment of the upper ocean (d1) from Myhre et al. (2013), rather than from Millar et al. (2017). We are testing the model responses as they would be 'out of the box' and only make modifications if required for the models to run, as was the case for Hector v1.1 to handle a 4xCO_2 concentration step.

Here we included additional model responses from the AR5-IR model using parameters from Millar et al. (2017). The parameter choices are available below in Table S2.

Table S2 Parameter values for the simple impulse-response model, AR5-IR

Parameter (Units)	Value – AR5-IR (from Myhre et al., 2013)	Value – AR5-IR-var (from Millar et al., 2017)	Guiding analogues
α (Wm^{-2})	5.35	5.395 (α = F2x/ln(2); F2x=3.74)	CO_2 RF scaling parameter
q_1 ($KW^{-1}m^2$)	0.631	0.41	Thermal adjustment of the upper ocean
q_2 ($KW^{-1}m^2$)	0.429	0.33	Thermal equilibrium of the deep ocean
d_1 (year)	8.4	4.1	Thermal adjustment timescale of the upper ocean
d_2 (year)	409.5	239.0	Thermal equilibrium timescale of the deep ocean

Figure S1 shows the temperature response from a CO_2 concentration impulse and Figure S2 shows the temperature response from a CO_2 concentration step in several SCMs, including the AR5-IR response found using the Millar et al. (2017) time constants, which we refer to as "AR5-IR-Millar-parameters" in this figure. We note that the AR5-IR-parameters response is still not identical to FAIR because FAIR has a differential response to changing background CO_2 concentrations.

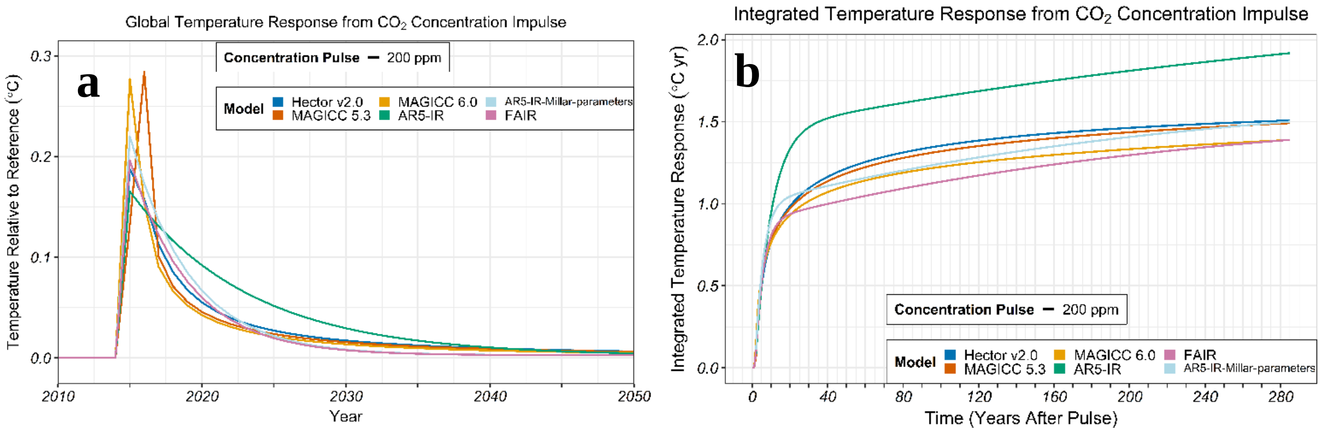

Figure S1 *Global mean temperature response (a) and integrated global mean temperature response (b) from a CO_2 concentration perturbation in SCMs (MAGICC 6.0 – yellow, MAGICC 5.3 BC-OC – red, Hector v2.0 – blue, AR5-IR – green, FAIR –pink, AR5-IR-Millar-parameters –light blue). The time-integrated response, analogous to the Absolute Global Temperature Potential, is reported as 0-285 years after the perturbation.*

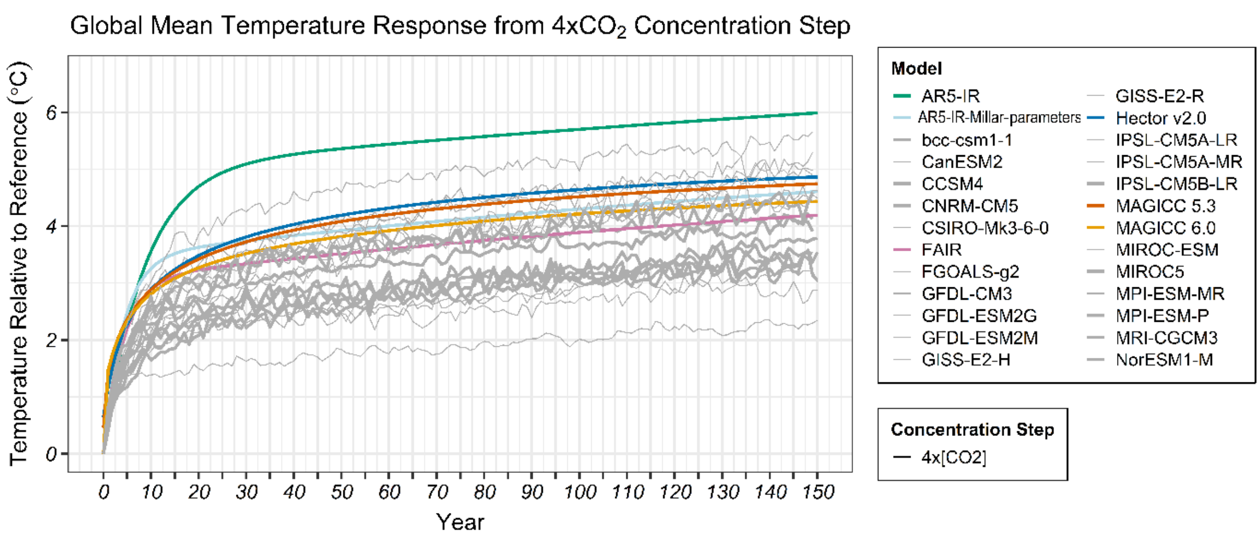

Figure S2 *Global mean temperature response from $4xCO_2$ concentration step in CMIP5 models (grey) and SCMs (MAGICC 6.0 – yellow, MAGICC 5.3 BC-OC – red, Hector v2.0 – blue, FAIR – pink, AR5-IR – green, AR5-IR-Millar-parameters – light blue). A climate sensitivity value of 3°C was used in the SCMs and the thick lines represent CMIP5 models with an ECS between 2.5 - 3.5 °C.*

We note that, while the Millar et al. (2017) parameters in Table S2 may provide a better short-term fit, they underestimate the long-term response of the ocean. The long-term ocean thermal time scale, which can only be estimated using multi-century model runs, is known to be longer than 200 years from basic physical principles (as seen in the original literature cited by the AR5 model, which used longer model runs to inform those parameters). While this may be an acceptable tradeoff if this model is only going to be used over a 100-year timescale, this will inevitably lead to bias on longer time-scales. The simple climate models tested in this study are used for a variety of purposes and over a range of time-scales. This illustrates why we use the original parameters of the models as set by their designers.

S2.4 MAGICC 5.3 BC-OC

MAGICC 5.3 BC-OC is a version of MAGICC 5.3 developed in conjunction with the Global Change Assessment Model (GCAM). MAGICC 5.3 used here is available in GCAM version 4.4, available for download at https://github.com/JGCRI/gcam-core/releases. The major change in this version of MAGICC was the addition of explicit BC and OC (Smith and Bond, 2014). To enable MAGICC 5.3 within GCAM, the climate model must be set to <Value name = "climate">../input/climate/magicc.xml</Value> within the configuration file. We ran this model with all its default configuration settings unless otherwise noted in the text. We reiterate that all model parameters and input files are provided in the Supplementary Materials.

S2.5 MAGICC 6.0

MAGICC 6.0 was run with all the default settings. For the main experiments, the climate sensitivity was set to 3.0°C to match the default setting of MAGICC 5.3 BC-OC and Hector v2.0, unless otherwise noted. The MAGICC 6.0 executable is available for free download here: http://www.magicc.org/. We reiterate that all model parameters and input files are provided in the Supplementary Materials.

S2.6 Hector v2.0 Settings

In the version we use here, Hector (v2.0), is coupled to a 1-D diffusive heat and energy balance model (DOECLIM: Diffusion Ocean Energy balance CLIMate model). We are using the 1-D diffusive ocean heat component of DOECLIM. DOECLIM is well documented and has been widely used in climate uncertainty studies (Bakker et al., 2017; Kriegler, 2005; Urban et al., 2014). Using default Hector parameter values for climate sensitivity and heat diffusivity, we find that the new coupled model (Hector v2.0) exhibits improved vertical ocean structure and heat uptake, as well as surface temperature response to radiative forcing, compared to earlier versions of Hector. We reiterate that all model parameters and input files are provided in the Supplementary Materials.

S3 CMIP5 Model Data

The CMIP5 model data used to produce Figure 4 is described here. Raw climate model output from 20 models was obtained from the CMIP5 data archive (http://cmip-pcmdi.llnl.gov/cmip5/data_portal.html) and the World Data Center for Climate site (http://cera-www.dkrz.de/WDCC/ui/Index.jsp). The monthly temperature data is aggregated to the global annual mean level using code developed using CDOs (see CDO 2018: Climate Data Operators. Available at http://www.mpimet.mpg.de/cdo). The long-term drift is removed from the CMIP5 model data by subtracting the linear trend from the corresponding pre-industrial control run (Gupta et al., 2013). Table S3 provides the CMIP5 modeling centre name and the model name from Figure 4.

Table S3 CMIP5 and SCM model information

Centre(s)	Model name
Beijing Climate Center (BCC) **China**	BCC-CSM1.1
Canadian Centre for Climate Modelling and Analysis (CCCma) **Canada**	CanESM2
National Center for Atmospheric Research **USA**	CCSM4

Centre National de Recherches Météorologiques, Centre Européen de Recherche et de Formation Avancée en Calcul Scientifique (CNRM-CERFACS) **France**	CNRM-CM5
Commonwealth Scientific and Industrial Research Organization/Queensland Climate Change Centre of Excellence **Australia**	CSIRO-Mk3-6-0
Institute of Atmospheric Physics, Chinese Academy of Sciences (LASG-CESS) **China**	FGOALS-g2
Geophysical Fluid Dynamics Laboratory (NCAR; NSF-DOE-NCAR) **USA**	GFDL-CM3
	GFDL-ESM2G
	GFDL-ESM2M
NASA/GISS (Goddard Institute for Space Studies; NASA-GISS) **USA**	GISS-E2-H
	GISS-E2-R
Institut Pierre Simon Laplace (IPSL) **France**	IPSL-CM5A-LR
	IPSL-CM5A-MR
	IPSL-CM5B-LR
Atmosphere and Ocean Research Institute (The University of Tokyo), National Institute for Environmental Studies, and Japan Agency for Marine-Earth Science and Technology (MIROC) **Japan**	MIROC-ESM
	MIROC5
Max Planck Institute for Meteorology (MPI-M) **Germany**	MPI-ESM-MR
	MPI-ESM-P
Meteorological Research Institute **Japan**	MRI-CGCM3
Norwegian Meteorological Institute **Norway**	NorESM1-M

S3.1 Abrupt 4xCO_2 concentration step response from Geoffroy et al. (2013)

Conducting impulse tests with complex models is computationally expensive, illustrated by the few studies employing this technique to understand the responses of models. We cite the Sand et al. (2016) study that specifically investigated NorESM's response to black carbon (BC) perturbations (Sand et al., 2016). Another study by Yang et al. (2019) conducted similar BC perturbations in CESM (Yang et al., 2019). Other stylized CMIP5 experiments, such as the 1% CO_2 concentration experiment, are not included in our comparison because we do not consider them to be impulse response tests. It is not possible to cleanly extract the impulse response from the 1% experiments. The CMIP5 4xCO_2 concentration step experiment is mathematically related to impulse responses, so are a reasonable comparison, particularly because these are the largest suite of such tests conducted in complex models, which is the reason we highlight these results in the paper.

Geoffroy et al. (2013) reported the 4xCO_2 concentration step temperature change relative to the 150-year temperature mean from the corresponding pre-industrial control run. For comparison to the simple models, we report the drift corrected 4xCO_2 concentration step temperature change relative to the start of the 4xCO_2 concentration run. Therefore, there will be a difference in the temperature reported.

Figure S3 shows the global mean temperature response from the 4xCO_2 concentration step experiment for the 20 CMIP5 models used in our comparison following the Geoffroy et al. (2013) procedure of reporting the 4xCO_2 concentration step temperature change relative to the 150-year temperature mean from the corresponding pre-industrial control run. The responses reported in Figure S3 are consistent with Geoffroy et al. (2013).

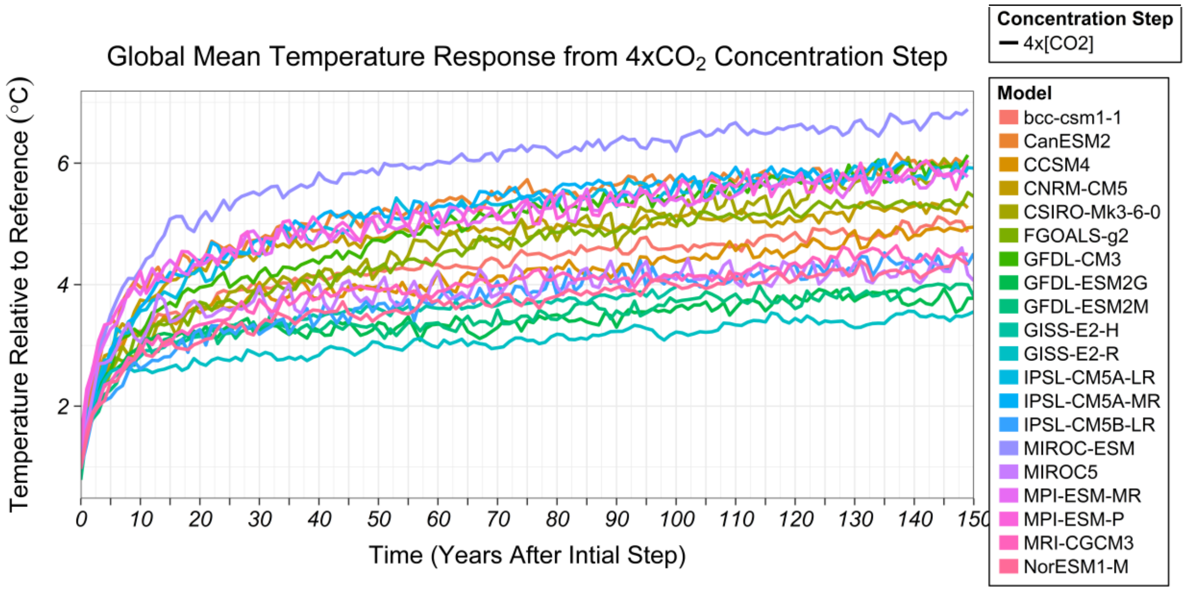

Figure S3 *Global mean temperature response from 4xCO_2 concentration step in CMIP5 models following the Geoffroy et al. methodology.*

S4 Sensitivity Experiments in MAGICC 5.3

We conduct two sensitivity experiments to illustrate there is little impact of these choices on the model responses: (1) perturb CO_2 emissions in different years and (2) perturb CO_2 emissions at different levels in 2015.

S4.1 Impact of Changes to the Years of Emission Impulses

We test CO_2 emissions perturbations in different years from the default 2015 used in the main text. Figure S4 shows the global mean temperature response normalized by the 2010 global mean temperature response from a CO_2 emissions pulse in MAGICC 5.3. We found a maximum of 0.028°C/PgC difference in the response in MAGICC 5.3 and, therefore, carried out the remainder of the experiment in 2015, avoiding model base years.

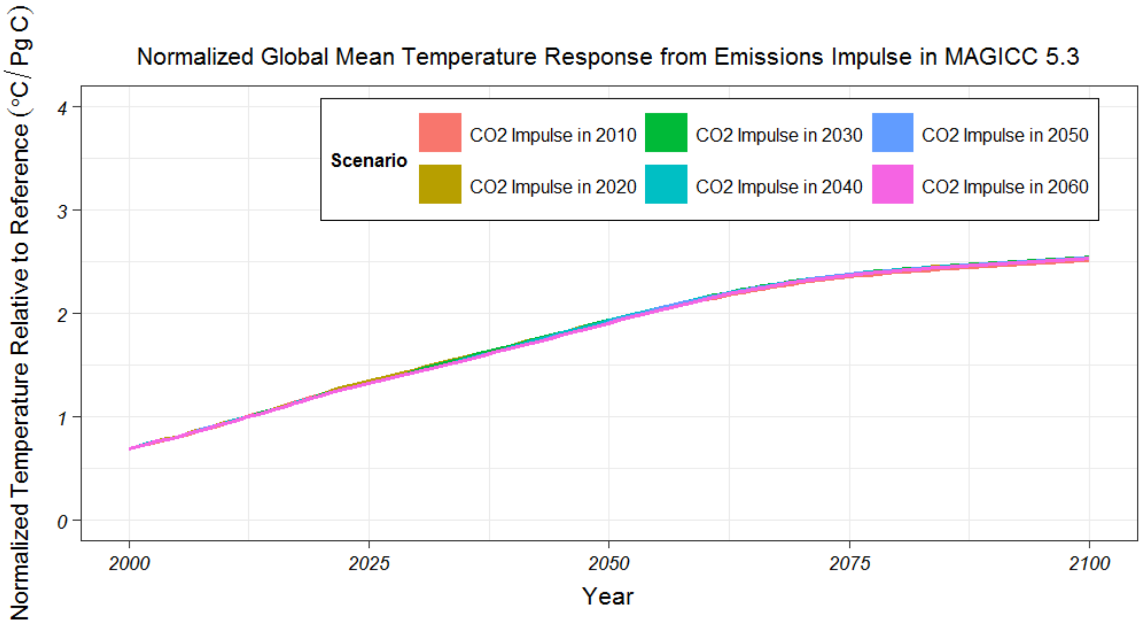

Figure S4 *Normalized global mean temperature response from CO_2 emissions impulses in MAGICC 5.3 carried out in different years.*

S4.2 Impact of Emissions Pulses Size on Temperature Response

In the main text, we carried out annual emissions perturbations equivalent to doubling the value in 2015 to avoid model base years. Figure S5 shows the global mean temperature response normalized by the perturbation size for different CO_2 perturbation sizes in 2015 in MAGICC 5.3. We found there was a maximum difference of 0.0015°C/PgC, and thus we continued our experiments using only one perturbation value.

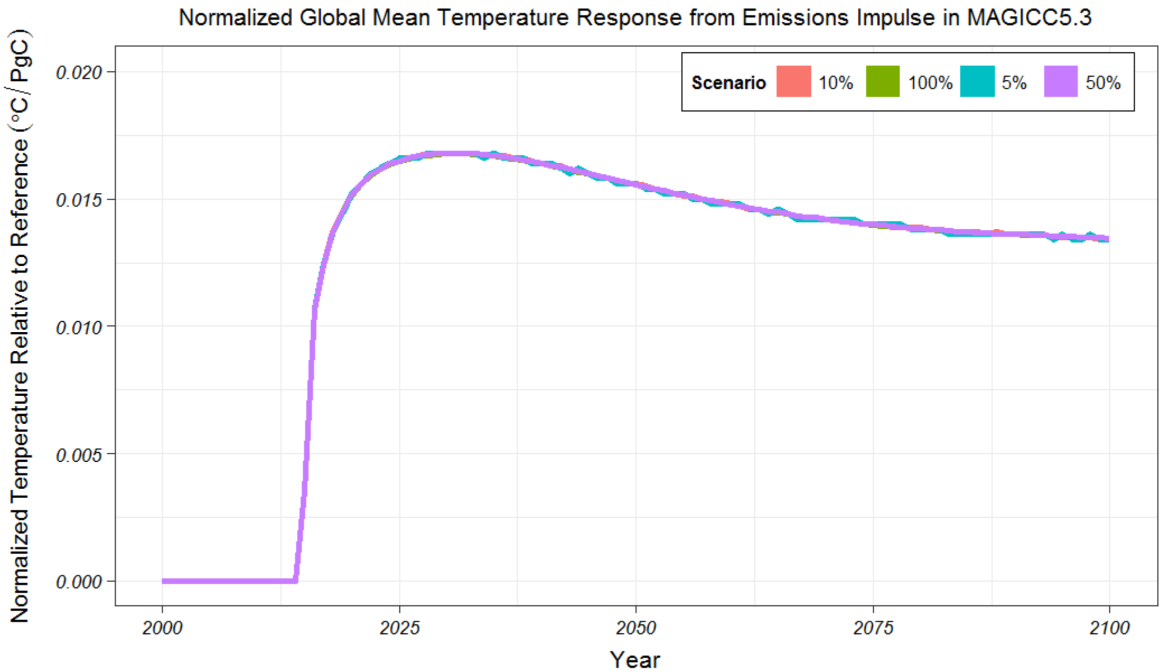

Figure S5 *Normalized global mean temperature response from different sized CO_2 emissions impulses in MAGICC 5.3 in 2015.*

S5 Adjusted Total Forcing Response

We found that MAGICC 5.3, MAGICC 6.0, and Hector v2.0 respond similarly to a CO_2 concentration impulse, with differences in the forcing and temperature responses arising from the treatment of time within each model. Hector v2.0, for example, reads in annual average emissions and carries out calculations using that same classification of time. MAGICC 5.3 and MAGICC 6.0 read in annual emissions and interpolate to obtain mid-year and end-of-year values and uses those internally to calculate concentration, forcing, and temperature at mid-year values, and successively reports temperature at the end-of-year. This change in the timing affects the impulse response by distributing the pulse over more time periods. Here, we demonstrate the impact of the adjustment for the forcing response to a CO_2 concentration impulse.

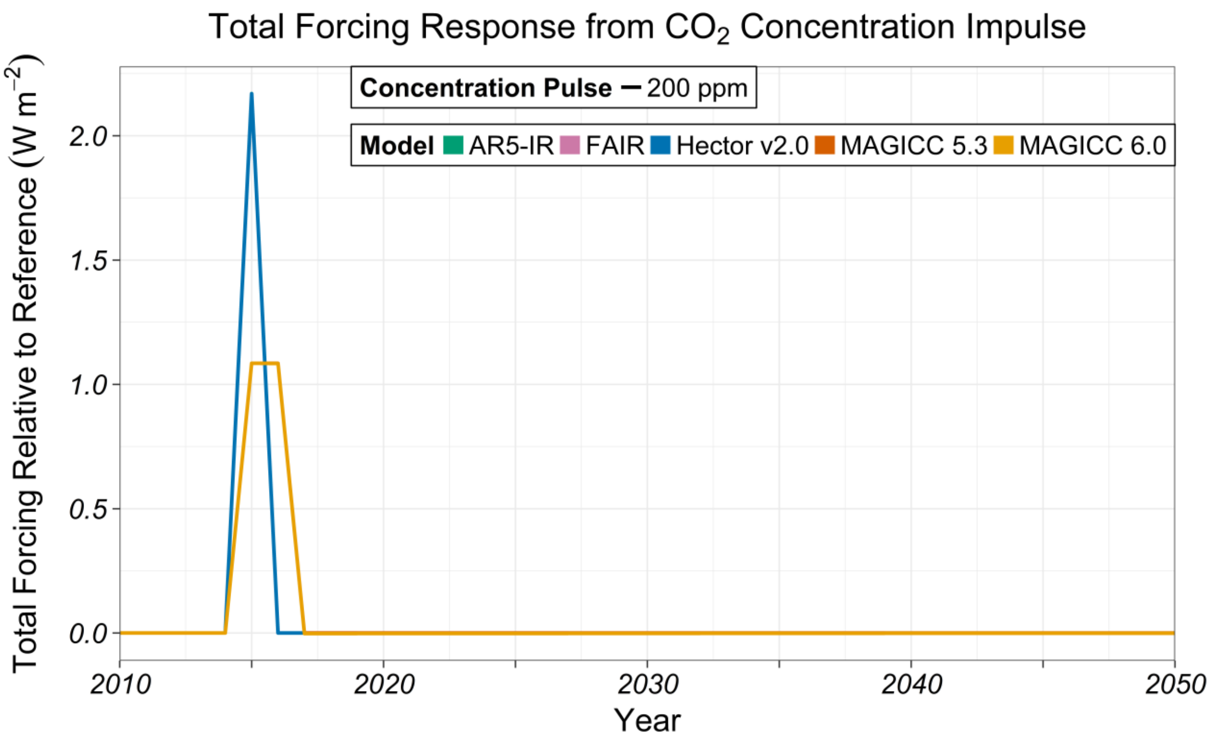

Figure S6 *Total forcing response from a CO_2 concentration impulse in SCMs. Three comprehensive SCMs have a collinear response (MAGICC 6.0 – yellow, MAGICC 5.3 BC-OC – red, Hector v2.0 – blue). The responses are co-linear past 2016.*

Due to the differences in model treatment of time, we offer a correction to the forcing in two of the SCMs. MAGICC 5.3 and MAGICC 6.0 calculate forcing in mid-year, while Hector v2.0 reports forcing at the end of a year. The result is a broadened impulse response peak in both versions of MAGICC, compared to Hector v2.0. The total forcing response from both version of MAGICC, however, can be adjusted with the following equation:

$$F_i = (2x f_i) - f_{i-1} \tag{11}$$

where F_i is the adjusted forcing, f_i is the unadjusted forcing at the current time step, and f_{i-1} is the unadjusted forcing at the previous time step.

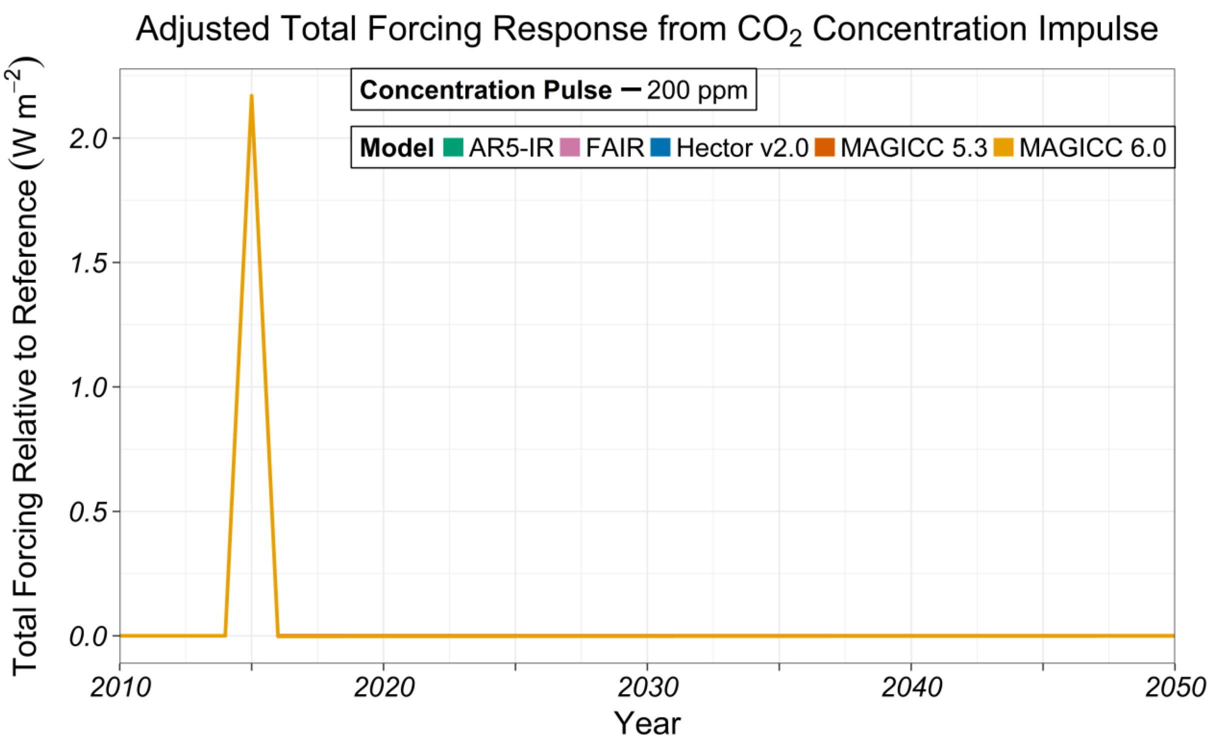

Figure S7 *Total forcing response from a CO_2 concentration impulse in SCMs. All three SCMs have a collinear response (MAGICC 6.0 – yellow, MAGICC 5.3 BC-OC – red, Hector v2.0 – blue, AR5-IR – green, FAIR –pink).*

Figure S7 shows the total forcing response adjusted from mid-year reporting to end-year reporting using equation (Eqn. S11). We can also apply this adjustment to the BC impulse, however, the MAGICC 6.0 distribution is larger in this case because MAGICC 6.0 annual emissions are interpolated to produce end-of-year and intermediate values. An annual emissions pulse is effectively spread over two model years. In the main paper, we report the integrated response because over these periods, the timing of the internal model calculations has minimal impact on the model results. Additional integrated model responses are in S9.

S6 Total Forcing Response from BC Emissions Impulse

We see in Figure S8 that the model responses to a pulse of BC have similar patterns of instantaneous behavior seen in Figure 1 from the CO_2 concentration pulse. In general, the models behave similarly in response to a BC pulse; Hector v2.0 and AR5-IR have a collinear response, while MAGICC 6.0 distributes the BC emissions pulse over 3 years.

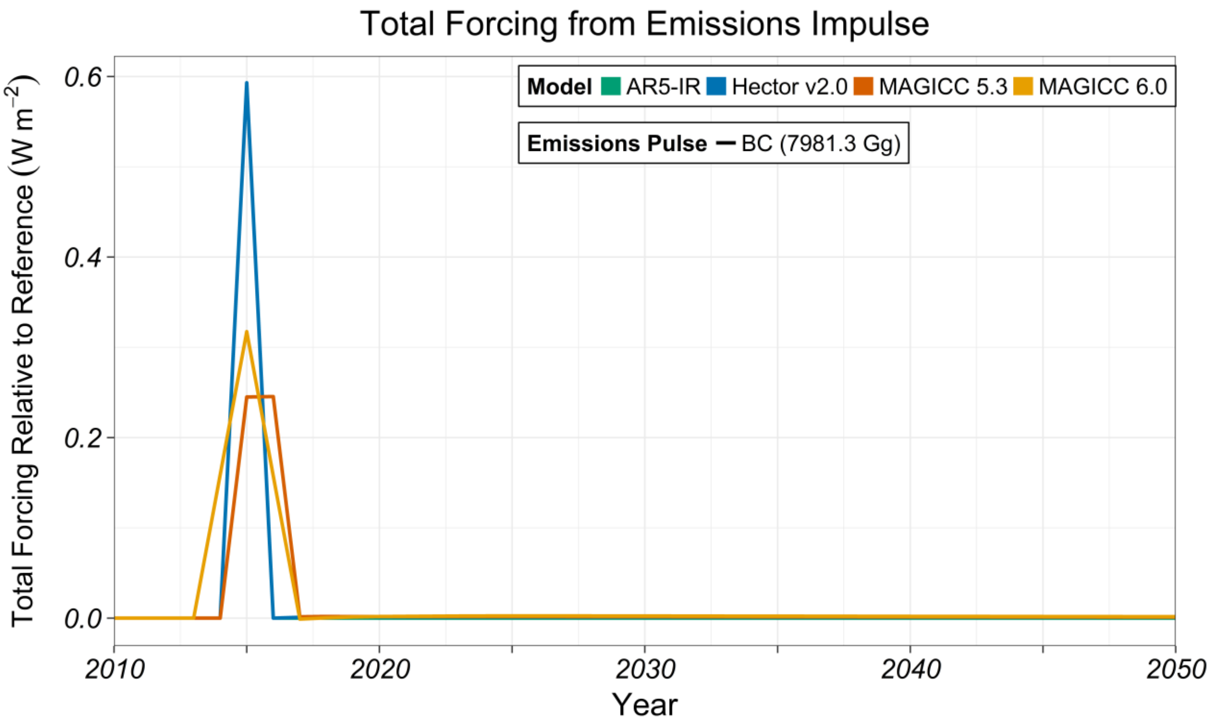

Figure S8 *Total forcing response from a BC emissions perturbation in SCMs (MAGICC 6.0 – yellow, MAGICC 5.3 BC-OC – red, Hector v2.0 – blue, AR5-IR-green). AR5-IR and Hector v2.0 are collinear.*

S7 CO_2 Concentration Responses from Emissions Impulses

Figure S9 shows the CO_2 concentration responses from a BC and CH_4 emissions pulse. Every model response shows an eventual CO_2 concentration increases from a BC impulse; a feedback from the temp increase impact on the carbon cycle. From a CH_4 and BC emissions pulse, the CO_2 concentration response is stronger in MAGICC 6.0, followed by MAGICC 5.3 and Hector v2.0. MAGICC 6.0, however, shows an initial decrease in CO_2 concentration response from the BC pulse.

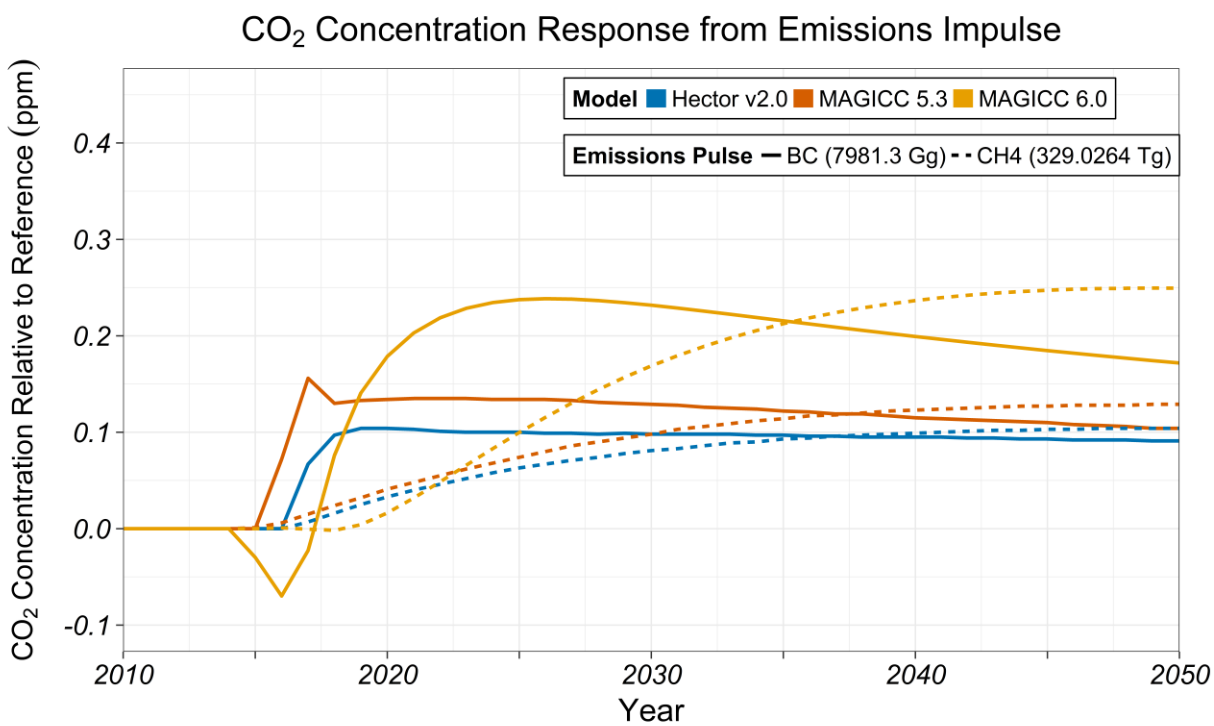

Figure S9 *CO_2 concentration response from CH_4 and BC emissions perturbation (B) in SCMs (MAGICC 6.0 – yellow, MAGICC 5.3 BC-OC – red, Hector v2.0 – blue) illustrating the carbon-cycle feedbacks present in each model.*

Figure S9 also shows that CH_4 emission perturbations impact CO_2 concentration within both versions of MAGICC. The discrepancy between the MAGICC and Hector responses is partly due to CH_4 oxidation in MAGICC 5.3. The MAGICC 6.0 response is larger in Figure S9 presumably due to feedback effects in the model, however, the general shape of the response is similar to the other two SCMs.

AR5-IR is notably absent from Figure S9 because, in this IRF model, the CO_2 concentrations are not affected by changing temperature (Millar et al., 2017). Rising temps in general and including temp changes due to CH_4 and BC emissions perturbations. FAIR v1.0 model (Millar et al., 2017) is absent from Figure S9 because the model does not report out the internally-calculated forcing response. The CO_2 concentration response to a CO_2 emissions impulse in FAIR can be seen in Figure S11.

The CH_4 chemistry components in Hector v2.0 and MAGICC 5.3 BC-OC are nearly identical, accounting for the similarities between these two SCMs responses (Hartin et al., 2015). MAGICC 5.3, however, includes CH_4 oxidation to CO_2, which might account for this response difference. To test this, Figure S10 shows the CO_2 concentration response from emissions impulse in SCMs. MAGICC 5.3 is shown with and without CH_4 oxidation included for a clearer comparison of the Hector v2.0 response. With the CH_4 oxidation turned off, the MAGICC 5.3 BC-OC response is similar to Hector v2.0 with only a slight difference after 2025.

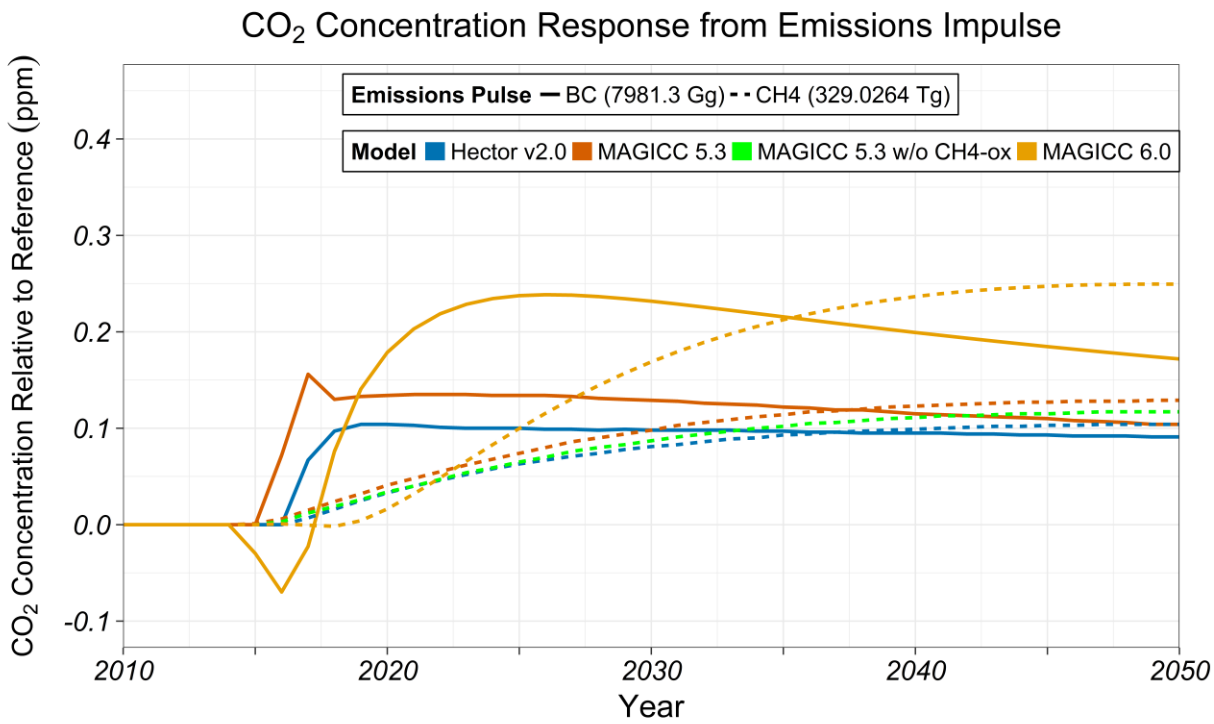

Figure S10 *CO_2 concentration response from emissions impulse in SCMs. MAGICC 5.3 is shown with and without CH_4 oxidation included (MAGICC 6.0 – yellow, MAGICC 5.3 BC-OC – red, Hector v2.0 – blue)..*

S8 Model Responses out to 2300

Figure S11 - Figure S15 show the CO_2 concentration response, total forcing response, and global mean temperature response from an emissions impulse, respectively, to the end of the model period equal to 2300.

S8.1 CO_2 Concentration Response to a CO_2 Emissions Pulse

Figure S11 shows the CO_2 concentration response from a CO_2 emissions pulse in the SCMs out to 2300. We see that the SCMs respond similarly to this perturbation, with the exception of the idealized SCM, FAIR, which has a weaker response.

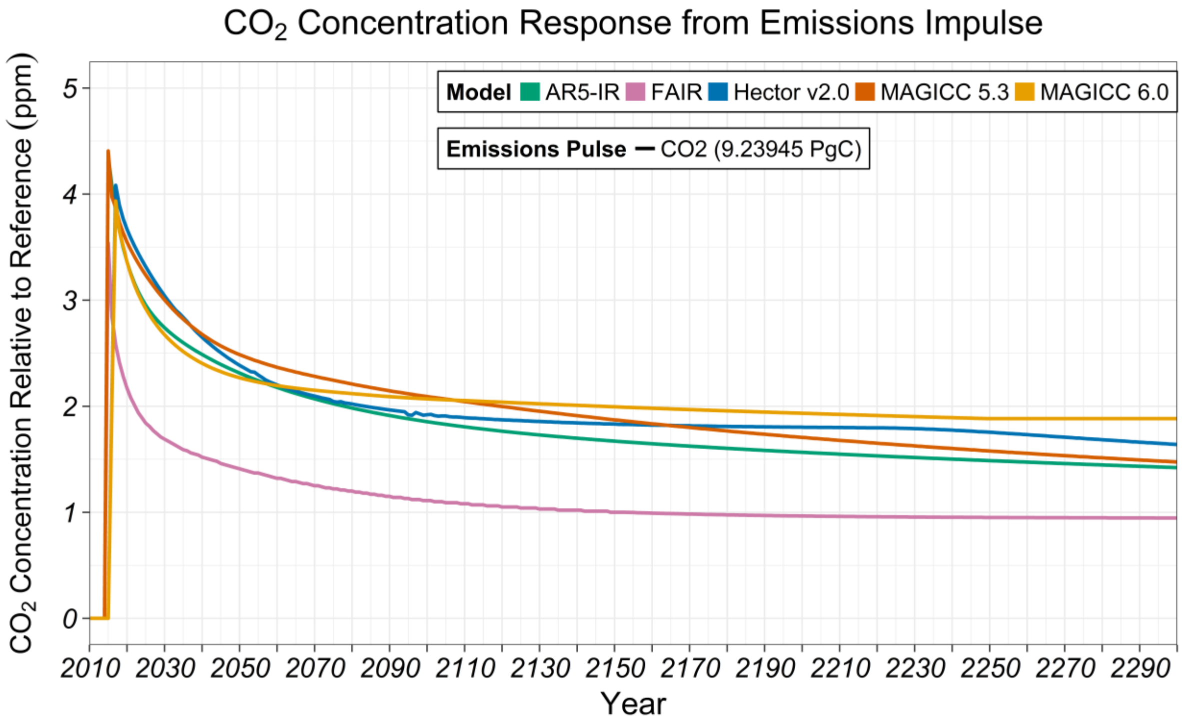

Figure S11 *Carbon dioxide concentration response from a CO_2 emissions pulse in SCMs (MAGICC 6.0 – yellow, MAGICC 5.3 BC-OC – red, Hector v2.0 – blue, AR5-IR – green, FAIR - pink).*

S8.2 CH_4 Concentration Response from CH_4 Emissions Pulse

Figure S12 shows the CH_4 concentration response from a CH_4 emissions pulse in the comprehensive SCMs out to 2300. The idealized SCMs do not report CH_4 concentrations. We see that the comprehensive SCMs behave similarly in their response to this perturbation, especially after 2050 when the response tends towards 0 ppb.

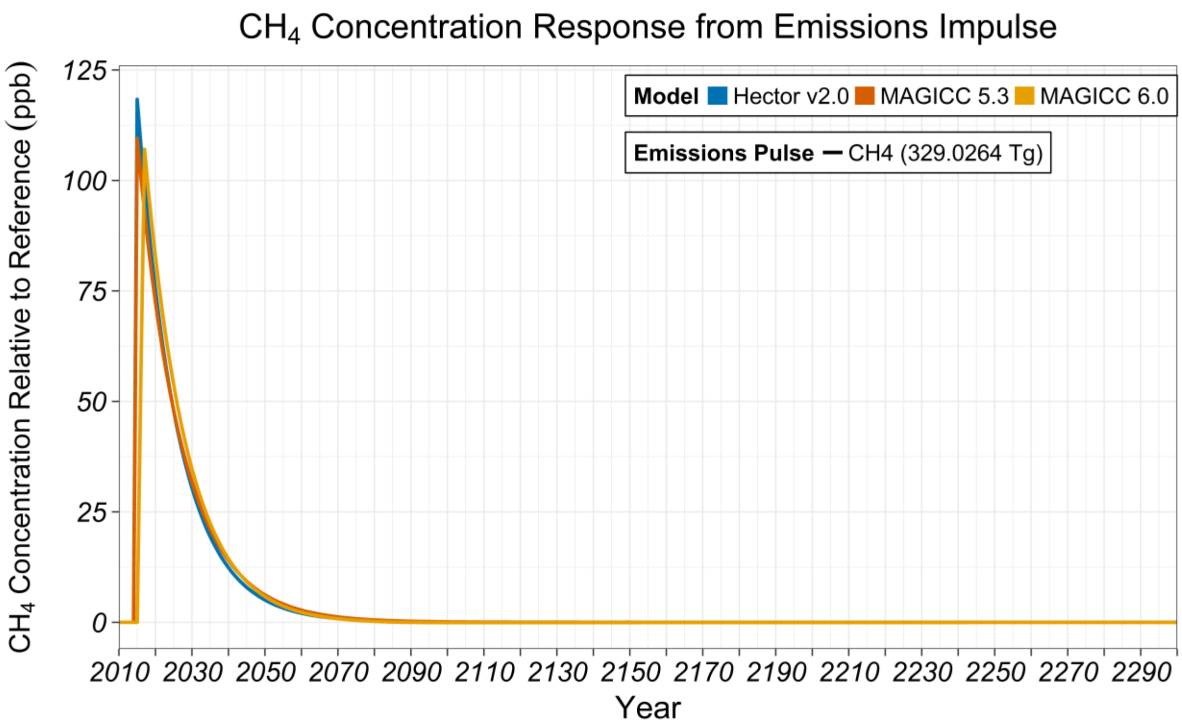

Figure S12 *Methane concentration response from a CH_4 emissions pulse in SCMs out to 2300 (MAGICC 6.0 – yellow, MAGICC 5.3 BC-OC – red, Hector v2.0 – blue).*

S8.3 CO_2 Concentration Response to a BC or CH_4 Emissions Pulse

Figure S13 shows the CO_2 concentration response from a CH_4 and BC emissions perturbations in the SCMs out to 2300. We see that the SCMs behave differently across the entire time series. Hector v2.0 appears to change state after 2225.

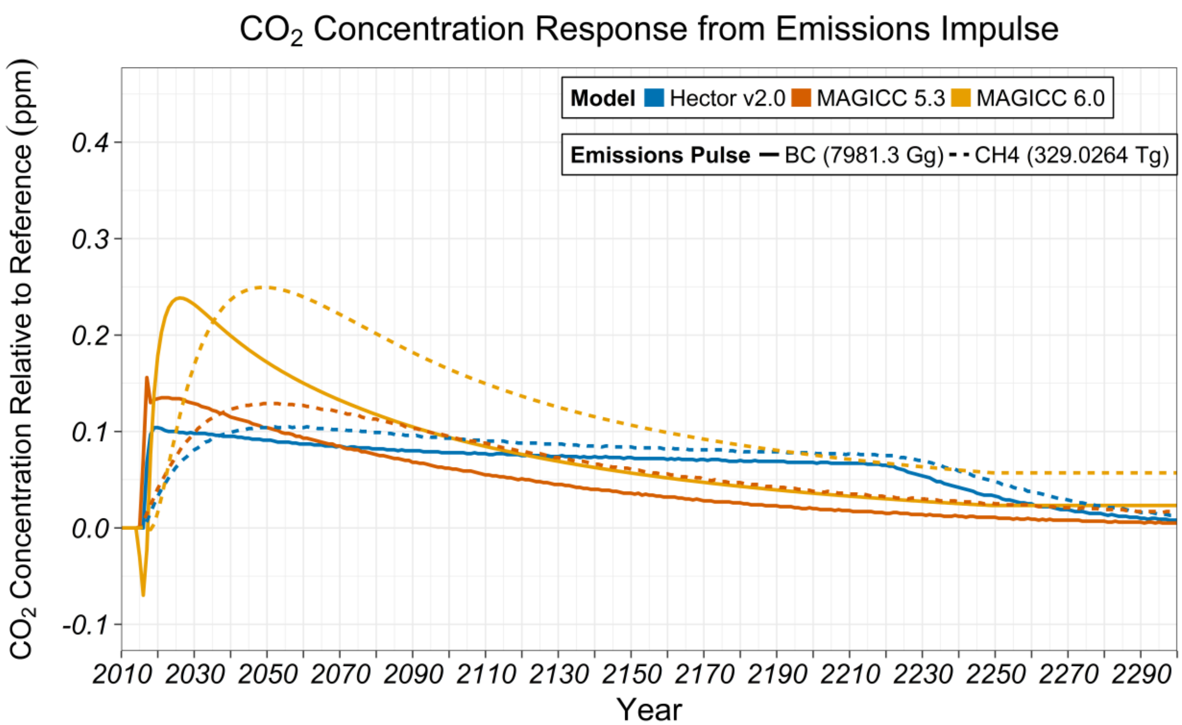

Figure S13 *CO_2 concentration response from emissions perturbations in SCMs out to 2300 (MAGICC 6.0 – yellow, MAGICC 5.3 BC-OC – red, Hector v2.0 – blue).*

S8.4 Total Forcing Response to a CO_2 or CH_4 Emissions Pulse

We report the total forcing response from the models, rather than the individual species' forcing responses for comparability. Additionally, the total forcing is similar to the individual forcing responses because forcing is dominated by the forcing from the perturbed species.

Figure S14 shows the total forcing response from a CH_4 and CO_2 emissions perturbations in the SCMs out to 2300. FAIR does not report total forcing.

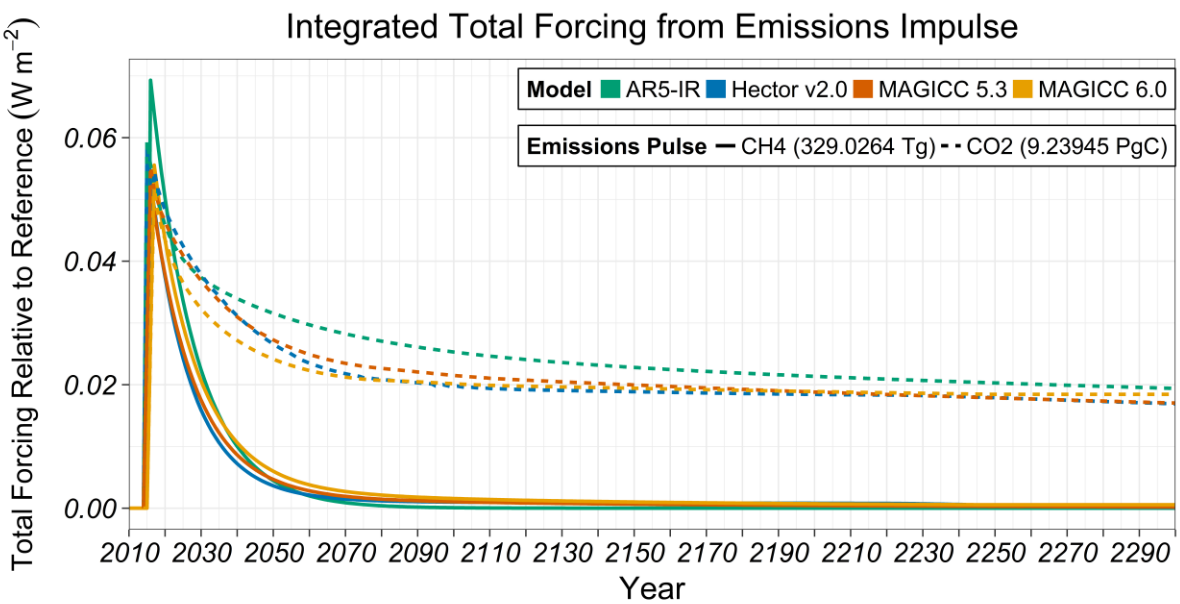

Figure S14 *Total forcing response from emissions perturbations in SCMs out to 2300 (MAGICC 6.0 – yellow, MAGICC 5.3 BC-OC – red, Hector v2.0 – blue, AR5-IR – green).*

S8.5 Global Mean Temperature Response to a CH_4 or CO_2 Emissions Pulse

Figure S15 shows the temperature response from a CH_4 and CO_2 emissions perturbations in the SCMs out to 2300. We see that most of the SCM responses differ slightly immediately following the perturbation, but converge over time. AR5-IR has a stronger response than the other SCMs immediately following the perturbation. More details are included in the main paper.

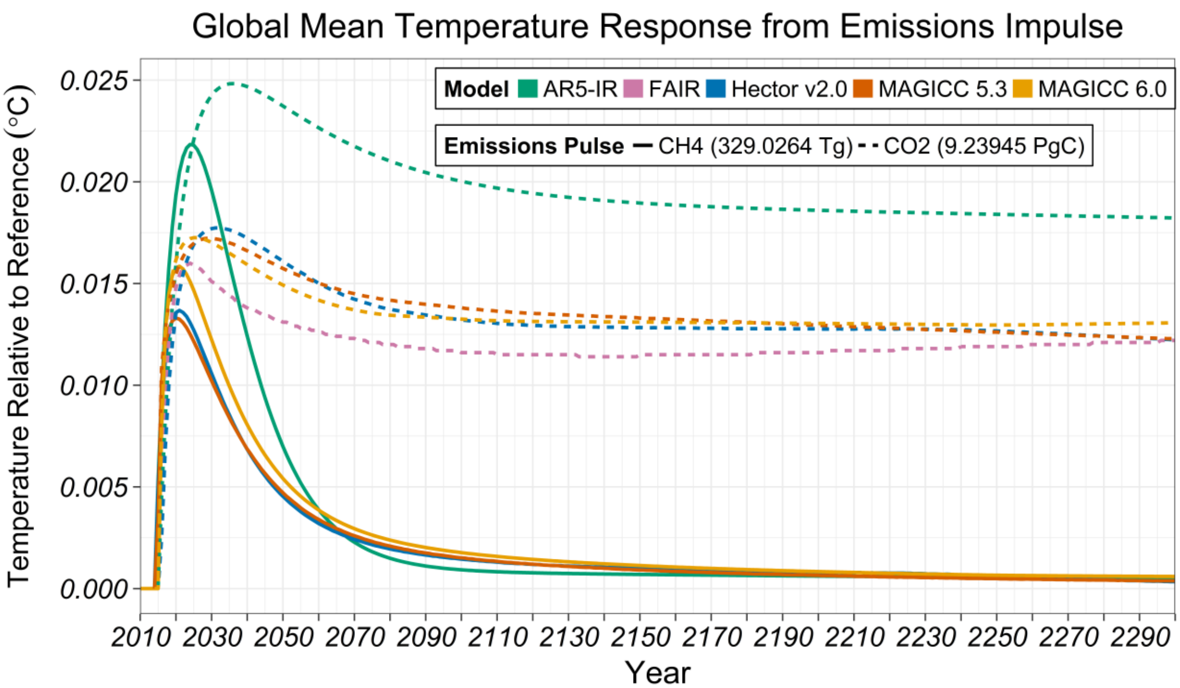

Figure S15 *Global mean temperature response from emissions perturbations in SCMs out to 2300 (MAGICC 6.0 – yellow, MAGICC 5.3 BC-OC – red, Hector v2.0 – blue, AR5-IR – green, FAIR - pink).*

S9 Time Integrated Responses

Figure S16 – Figure S21 shows the integrated forcing and temperature response for the full suite of experiments to the end of the model period. The data tables in this section provide numerical data (rounded to three significant figures) supporting the integrated forcing or temperature response figures. The data tables also include percent differences found using the following formula:

$$Percent\ Difference_{i,t} = \left(\frac{Model\ response_{i,t} - Average\ Comprehensive\ Model\ Response_t}{Average\ Comprehensive\ Model\ Response_t}\right) \times 100 \qquad (12)$$

where t is the time horizon and i is the individual model. A positive percent difference indicates that the model response is stronger than the average comprehensive model response, while a negative value indicates the model response was weaker than the average comprehensive model response.

S9.1 Time Integrated Responses from a CO_2 Concentration Impulse

Figure S16 shows the time-integrated total forcing response from a CO_2 concentration impulse.

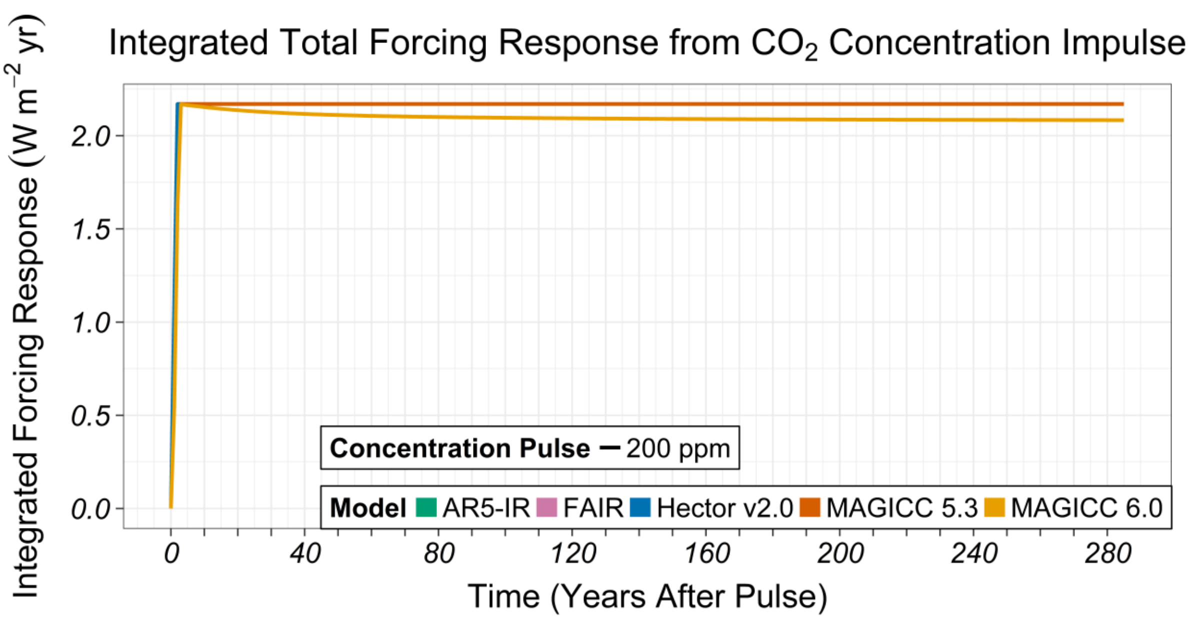

Figure S16 *Time-integrated forcing response from a CO_2 concentration impulse for the SCMs to the end of the model period (MAGICC 6.0 – yellow, MAGICC 5.3 BC-OC – red, Hector v2.0 – blue, AR5-IR – green, FAIR - pink).*

Figure S17 shows the time-integrated global mean temperature response from a CO_2 concentration impulse to the end of the model period. We see that the comprehensive SCMs respond similarly, while AR5-IR has a stronger response and FAIR, a slightly weaker response. The associated values time integrated temperature responses are in Table S4.

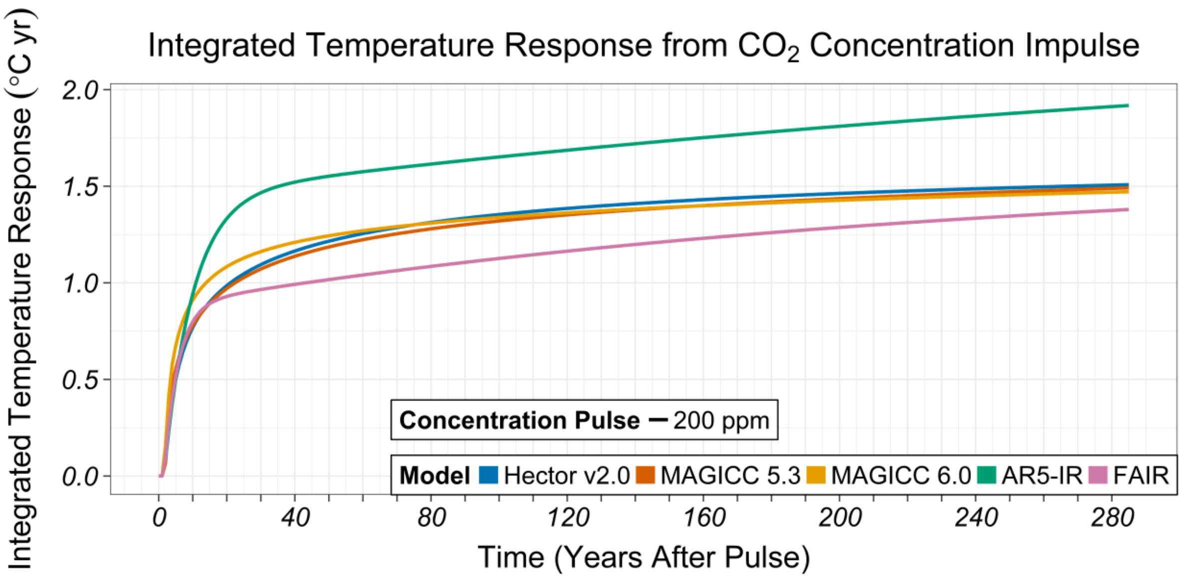

Figure S17 *Time-integrated temperature response from a CO_2 concentration impulse for the SCMs to the end of the model period (MAGICC 6.0 – yellow, MAGICC 5.3 BC-OC – red, Hector v2.0 – blue, AR5-IR – green, FAIR - pink).*

Table S4 Integrated Temperature Responses from a CO_2 Concentration Impulse in the SCMs

Time After Pulse	Integrated Temperature Response (°Cyr)						Percent Difference from Comprehensive SCMs Average (%)				
	MAGICC 5.3 BC-OC	MAGICC 6.0	Hector v2.0	FAIR	AR5-IR	Average of Comprehensive SCMs	MAGICC 5.3 BC-OC	MAGICC 6.0	Hector v2.0	FAIR	AR5-IR
10	0.85	0.98	0.85	0.87	0.24	0.90	-4.79	9.59	-4.79	-3.57	-73.5
20	1.00	1.11	1.02	0.94	1.10	1.04	-4.25	6.29	-2.04	-9.80	5.33
50	1.20	1.25	1.22	1.02	1.39	1.22	-2.07	2.26	-0.19	-16.6	13.7
100	1.32	1.34	1.35	1.13	1.65	1.34	-1.25	0.25	1.00	-15.5	23.4
150	1.39	1.39	1.42	1.13	1.74	1.40	-0.71	-0.71	1.43	-19.3	24.3
285	1.46	1.47	1.51	1.38	1.92	1.48	-1.31	-0.63	1.94	-6.71	29.8

S9.2 Time Integrated Responses from a CO_2 Emissions Impulse

Figure S18 and Figure S19 show the integrated forcing (Table S5) and temperature response (Table S6) for the CO_2 emissions impulse experiment to the end of the model period, respectively. The numerical data is shown in Table S5 and Table S6.

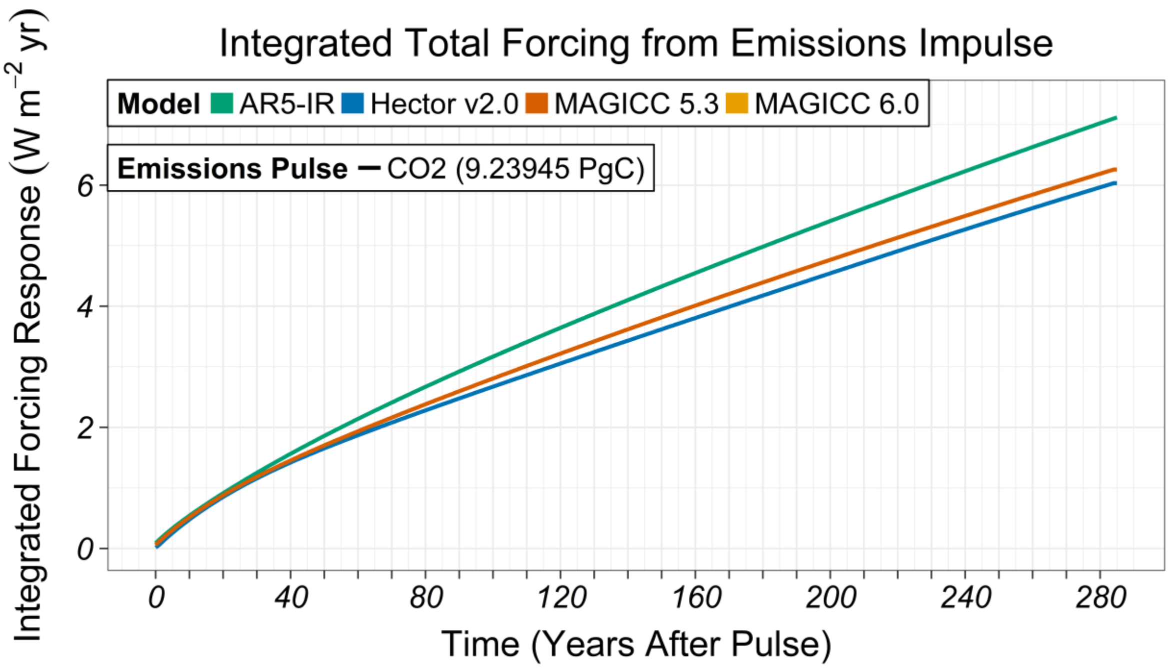

Figure S18 *Time-integrated total forcing response from a CO_2 emissions impulse for the SCMs to the end of the model period (MAGICC 6.0 – yellow, MAGICC 5.3 BC-OC – red, Hector v2.0 – blue, AR5-IR – green).*

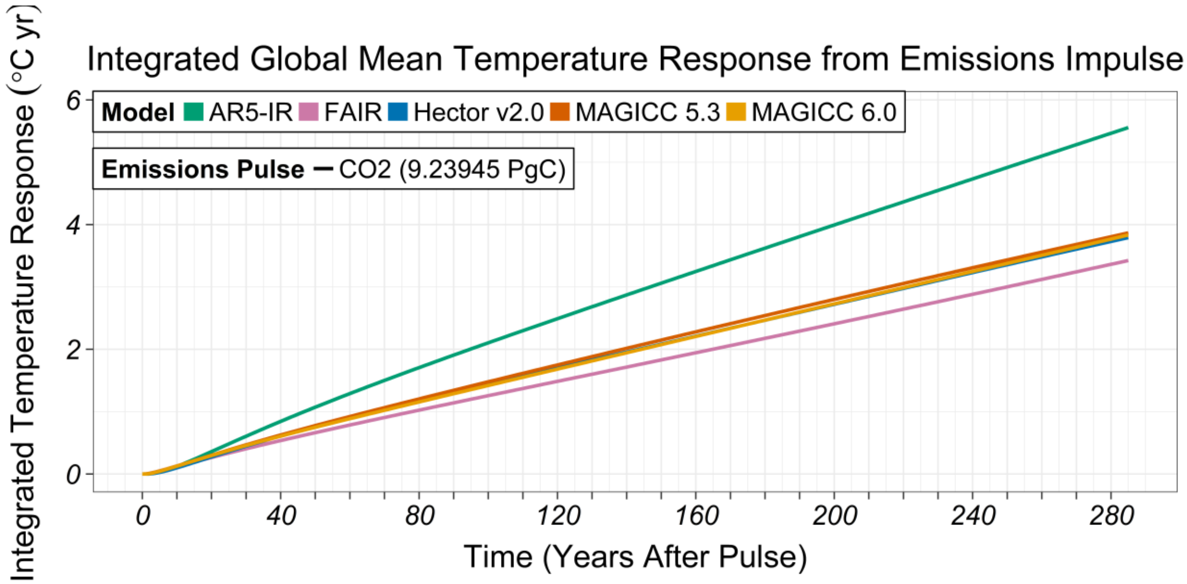

Figure S19 *Time-integrated temperature response from a CO_2 emissions impulse for the SCMs to the end of the model period (MAGICC 6.0 – yellow, MAGICC 5.3 BC-OC – red, Hector v2.0 – blue, AR5-IR – green, FAIR - pink).*

Table S5 Integrated Forcing Responses from a CO_2 Emissions Impulse in the SCMs

Time After Pulse	Integrated Forcing Response ($Wm^{-2}yr$)					Percent Difference from Comprehensive SCMs Average (%)			
	MAGICC 5.3 BC-OC	MAGICC 6.0	Hector v2.0	AR5-IR	Average of Comprehensive SCMs	MAGICC 5.3 BC-OC	MAGICC 6.0	Hector v2.0	AR5-IR
10	0.51	0.43	0.48	0.54	0.47	8.67	-9.51	0.85	14.38
20	0.88	0.75	0.85	0.91	0.82	6.39	-9.38	2.99	10.63
50	1.70	1.48	1.65	1.86	1.61	5.63	-8.28	2.65	15.38
100	2.81	2.50	2.67	3.17	2.66	5.52	-5.96	0.44	19.13
150	3.82	3.47	3.62	4.32	3.63	4.97	-4.52	-0.45	18.87
285	6.26	5.97	6.03	7.12	6.09	2.79	-1.89	-0.90	16.98

Table S6 Integrated Temperature Responses from a CO_2 Emissions Impulse in the SCMs

Time After Pulse	Integrated Temperature Response (°Cyr)						Percent Difference from Comprehensive SCMs Average (%)				
	MAGICC 5.3 BC-OC	MAGICC 6.0	Hector v2.0	FAIR	AR5-IR	Average of Comprehensive SCMs	MAGICC 5.3 BC-OC	MAGICC 6.0	Hector v2.0	FAIR	AR5-IR
10	0.16	0.16	0.13	0.14	0.18	0.15	6.81	5.49	-12.31	-5.71	20.66
20	0.33	0.33	0.31	0.29	0.42	0.32	2.99	1.44	-4.43	-9.38	29.90
50	0.81	0.78	0.79	0.69	1.00	0.79	1.86	-1.69	-0.17	-13.07	26.15
100	1.50	1.45	1.46	1.27	1.93	1.47	2.16	-1.59	-0.57	-13.51	31.44
150	2.17	2.10	2.10	1.85	2.86	2.12	2.20	-1.10	-1.10	-12.87	34.69
285	3.87	3.85	3.80	3.44	5.87	3.84	0.83	0.17	-1.00	-10.38	52.93

S9.3 Time Integrated Responses from a CH_4 Emissions Impulse

Figure S17 and Figure S18 show the integrated forcing (Table S6) and temperature response (Table S7) for the CH_4 emissions impulse experiment to the end of the model period. The numerical data in Table S6 and Table S7.

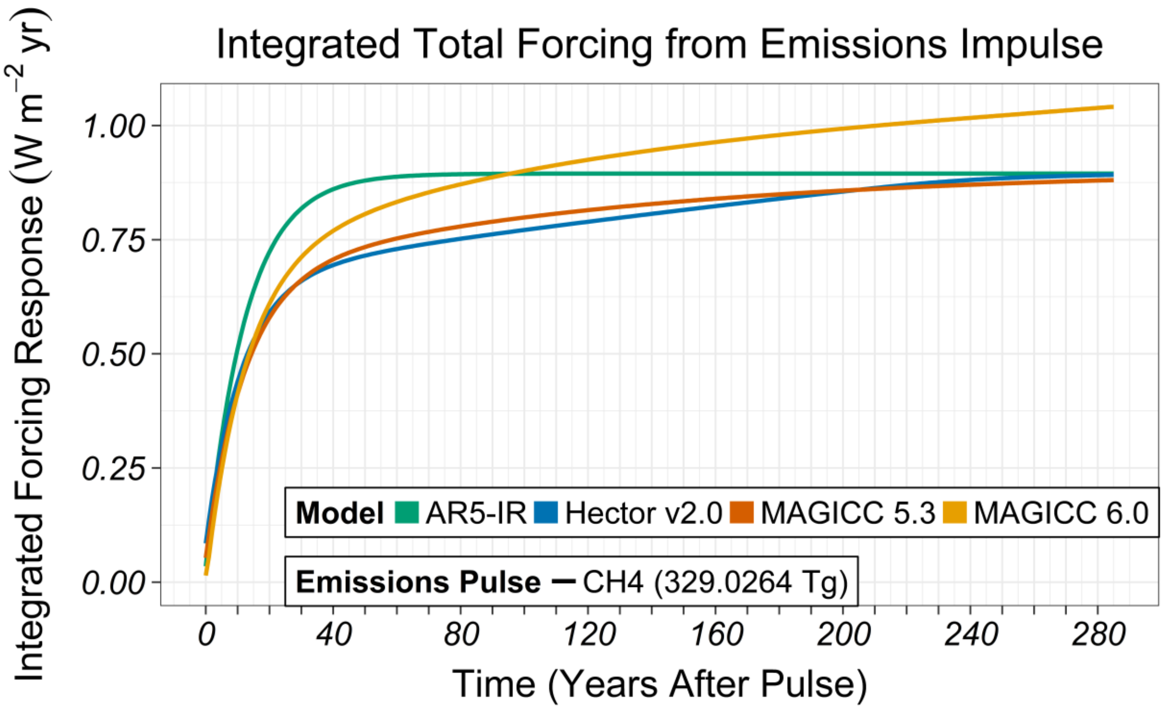

Figure S20 *Time-integrated total forcing response from a CH_4 emissions impulse for the SCMs to the end of the model period (MAGICC 6.0 – yellow, MAGICC 5.3 BC-OC – red, Hector v2.0 – blue, AR5-IR – green).*

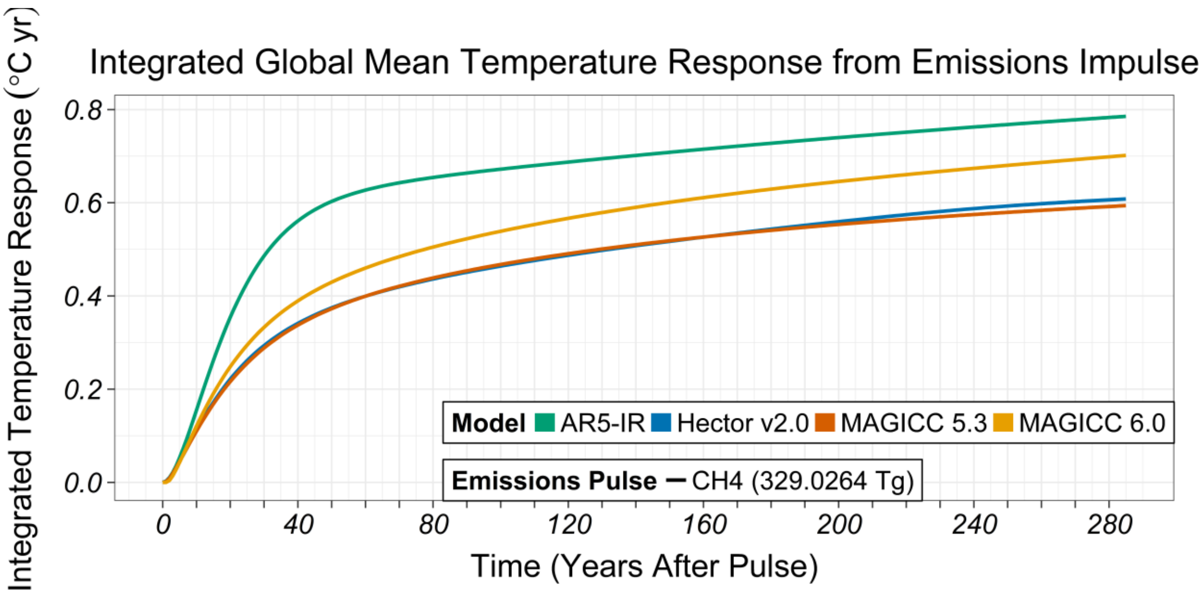

Figure S21 *Time-integrated temperature response from a* CO_2 *emissions impulse for the SCMs to the end of the model period (MAGICC 6.0 – yellow, MAGICC 5.3 BC-OC – red, Hector v2.0 – blue, AR5-IR – green, FAIR - pink).*

Table S7 Integrated Forcing Responses from a CH_4 Emissions Impulse in the SCMs

Time After Pulse	Integrated Forcing Response ($Wm^{-2}yr$)					Percent Difference from Comprehensive SCMs Average (%)			
	MAGICC 5.3 BC-OC	MAGICC 6.0	Hector v2.0	AR5-IR	Average of Comprehensive SCMs	MAGICC 5.3 BC-OC	MAGICC 6.0	Hector v2.0	AR5-IR
10	0.41	0.41	0.44	0.51	0.42	-2.14	-2.14	4.28	21.1
20	0.58	0.61	0.59	0.72	0.59	-2.31	2.76	-0.45	21.9
50	0.73	0.81	0.72	0.88	0.75	-2.44	7.28	-4.84	16.9
100	0.80	0.90	0.77	0.89	0.82	-3.04	9.36	-6.32	8.63
150	0.83	0.95	0.82	0.89	0.87	-3.88	9.95	-6.07	3.03
285	0.88	1.04	0.89	0.89	0.94	-6.01	10.9	-4.94	-4.62

Table S8 Integrated Temperature Responses from a CH_4 Emissions Impulse in the SCMs

Time After Pulse	Integrated Temperature Response (°Cyr)					Percent Difference from Comprehensive SCMs Average (%)			
	MAGICC 5.3 BC-OC	MAGICC 6.0	Hector v2.0	AR5-IR	Average of Comprehensive SCMs	MAGICC 5.3 BC-OC	MAGICC 6.0	Hector v2.0	AR5-IR
10	0.13	0.15	0.14	0.16	0.14	-4.26	7.10	-2.83	17.2
20	0.23	0.27	0.24	0.36	0.25	-5.56	8.68	-3.12	47.4
50	0.38	0.44	0.38	0.45	0.40	-5.03	9.55	-4.52	12.3
100	0.47	0.54	0.47	0.58	0.49	-4.54	9.88	-5.35	17.4
150	0.52	0.60	0.52	0.70	0.55	-4.99	10.2	-5.17	28.1
285	0.60	0.70	0.61	0.85	0.64	-6.20	10.5	-4.31	33.5

S9.4 Time Integrated Responses from a BC Emissions Impulse

Figure S19 and Figure S20 show the integrated forcing and temperature response for the BC emissions impulse experiment to the end of the model period, respectively. FAIR is not in this figure because we used FAIR v1.0, which only represented the response from CO_2 emissions. An updated version, FAIR v1.3, was recently released and includes non-CO_2 forcing. Table S8 shows the integrated temperature response data.

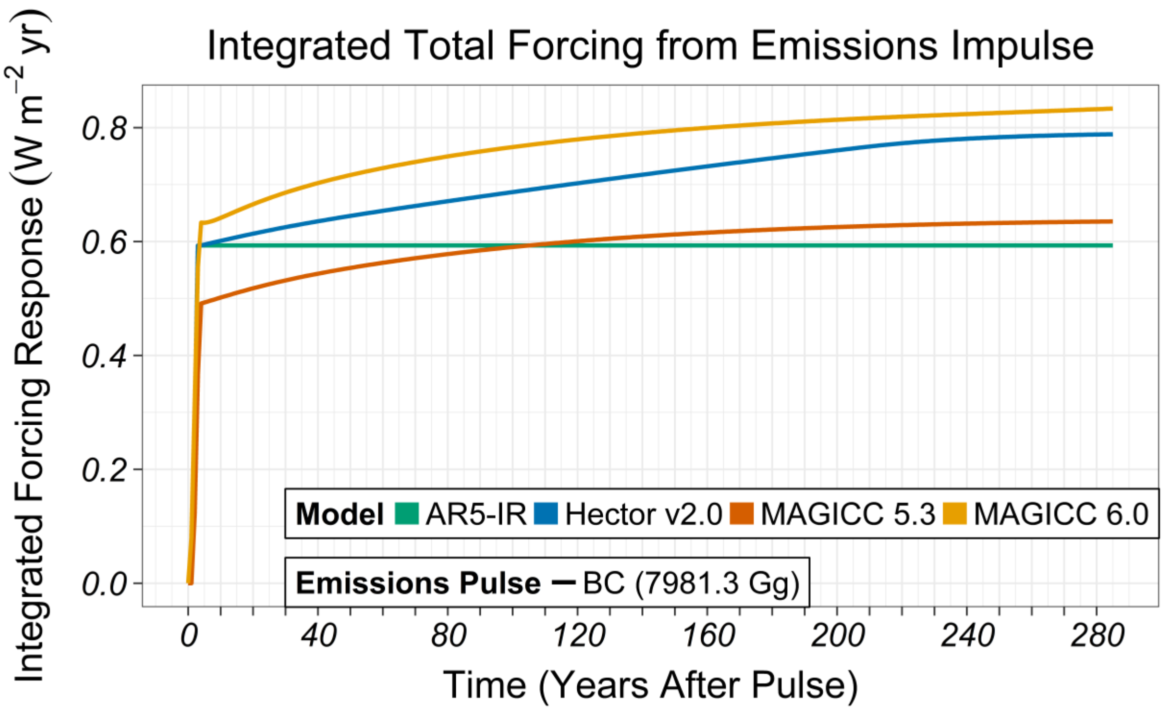

Figure S22 *Time-integrated total forcing response from a BC emissions impulse for the SCMs to the end of the model period (MAGICC 6.0 – yellow, MAGICC 5.3 BC-OC – red, Hector v2.0 – blue, AR5-IR – green).*

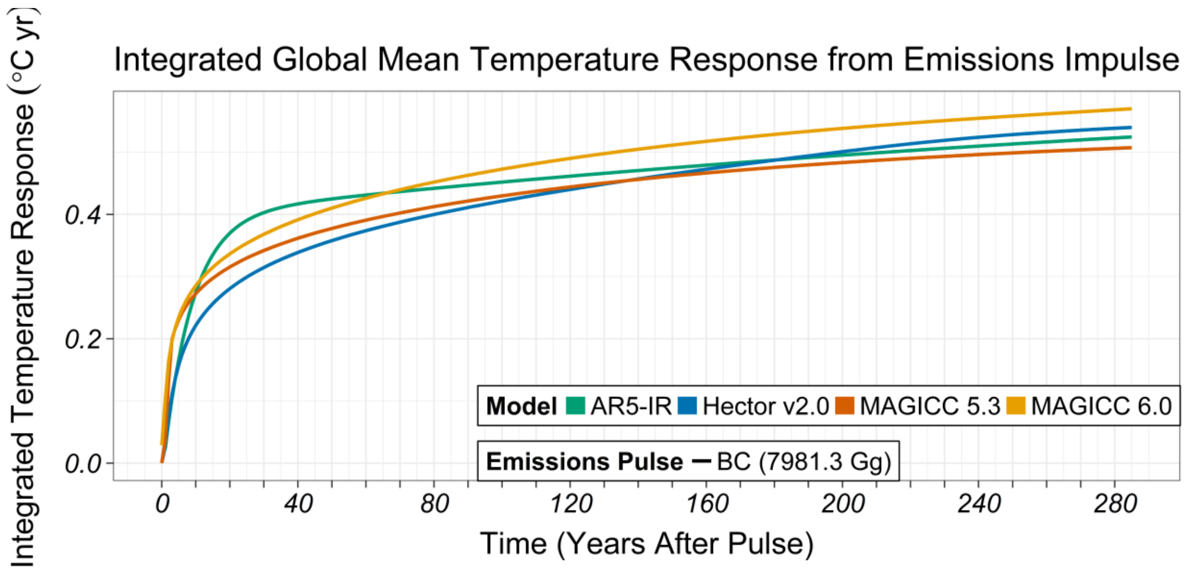

Figure S23 *Time-integrated temperature response from a BC emissions impulse for the SCMs to the end of the model period (MAGICC 6.0 – yellow, MAGICC 5.3 BC-OC – red, Hector v2.0 – blue, AR5-IR – green, FAIR - pink).*

We see that Hector v2.0, which does not differentiate BC forcing over land and ocean and has a 9% weaker response 20 years after the pulse. MAGICC 6.0 diverges from the MAGICC 5.3 temperature response 20 years after the pulse. AR5-IR represents the temperature response from a BC perturbation as a simple exponential decay analogous to the greenhouse gas IRF, leading to a much stronger integrated temperature response (20%) 20 years after the pulse.

Table S9 Integrated Temperature Responses from a BC Emissions Impulse in the SCMs

Time After Pulse	Integrated Temperature Response (°Cyr)					Percent Difference from Comprehensive SCMs Average (%)			
	MAGICC 5.3 BC-OC	**MAGICC 6.0**	**Hector v2.0**	**AR5-IR**	**Average of Comprehensive SCMs**	**MAGICC 5.3 BC-OC**	**MAGICC 6.0**	**Hector v2.0**	**AR5-IR**
10	0.28	0.30	0.24	0.30	0.27	3.91	9.22	-13.1	11.0
20	0.32	0.34	0.29	0.38	0.32	1.13	8.12	-9.25	19.3
50	0.38	0.41	0.36	0.43	0.38	-1.22	7.43	-6.21	10.7
100	0.43	0.47	0.42	0.45	0.44	-2.68	7.12	-4.44	2.22
150	0.46	0.51	0.47	0.48	0.48	-3.80	6.76	-2.96	-0.92
285	0.51	0.57	0.54	0.53	0.54	-5.90	5.73	0.17	-2.56

S10 Temporal Response of SCMs Compared to 4xCO2 Concentration Step Experiment from CMIP5

Here we compare the 20-year moving average at time t=30, t= 50, t=70, t=100, and t=130 in the CMIP5 models and SCMs to show the temporal response of temperature. Hector v2.0 and MAGICC 5.3 have a faster response than the other SCMs and the majority of the complex models to an abrupt $4xCO_2$ concentration step.

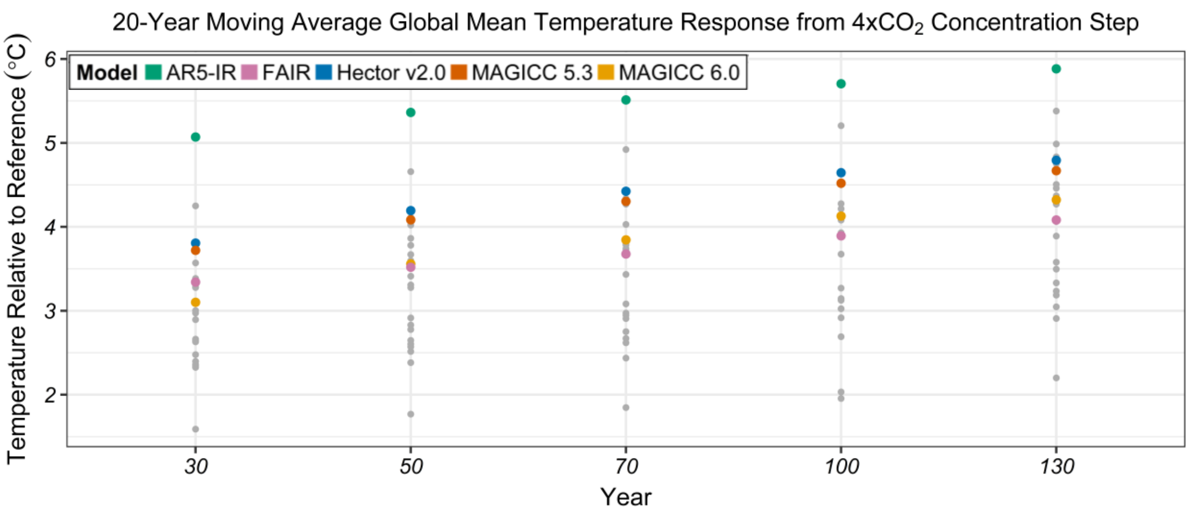

Figure S24 *20-Year moving average centered at year shown of the global mean temperature response from $4xCO_2$ concentration step in CMIP5 models (grey) and SCMs (MAGICC 6.0 – yellow, MAGICC 5.3 BC-OC – red, Hector v2.0 – blue, FAIR – pink, AR5-IR –green).*

Table S10 shows the ECS values and the realized warming fraction (RWF) for the CMIP5 data and SCMs used to produce Figure 4. The RWF reveals that the SCMs used in this study generally warm faster than the more complex models in CMIP5.

Table S10 *CMIP5 and SCM model information with ECS and RWF*

Centre(s)	Model name	ESC (°C)	RWF (%) $\sqrt{2}x\frac{Average\ of\ the\ last\ 40\ years}{ECS}$
Beijing Climate Center (BCC) **China**	BCC-CSM1.1	2.8	58
Canadian Centre for Climate Modelling and Analysis (CCCma) **Canada**	CanESM2	3.7	54
National Center for Atmospheric Research **USA**	CCSM4	2.9	51
Centre National de Recherches Météorologiques, Centre Européen de Recherche et de Formation Avancée en Calcul Scientifique (CNRM-CERFACS) **France**	CNRM-CM5	3.3	51
Commonwealth Scientific and Industrial Research Organization/Queensland Climate Change Centre of Excellence **Australia**	CSIRO-Mk3-6-0	4.1	47
Institut Pierre Simon Laplace (IPSL) **France**	IPSL-CM5A-LR	4.1	49
	IPSL-CM5A-MR	NA	--
	IPSL-CM5B-LR	2.6	54
Institute of Atmospheric Physics, Chinese Academy of Sciences (LASG-CESS) **China**	FGOALS-g2	NA	--
	MIROC-ESM	4.7	48

Atmosphere and Ocean Research Institute (The University of Tokyo), National Institute for Environmental Studies, and Japan Agency for Marine-Earth Science and Technology (MIROC) **Japan**	MIROC5	2.7	49
Max Planck Institute for Meteorology (MPI-M) **Germany**	MPI-ESM-MR	NA	--
	MPI-ESM-P	3.5	51
Meteorological Research Institute **Japan**	MRI-CGCM3	2.6	55
Norwegian Meteorological Institute **Norway**	NorESM1-M	2.8	48
NASA/GISS (Goddard Institute for Space Studies; NASA-GISS) **USA**	GISS-E2-H	2.3	49
	GISS-E2-R	2.1	44
Geophysical Fluid Dynamics Laboratory (NCAR; NSF-DOE-NCAR) **USA**	GFDL-CM3	4.0	52
	GFDL-ESM2G	2.4	57
	GFDL-ESM2M	2.4	65
Raper et al., 1996; Wigley and Raper 2002; Smith and Bond 2014	MAGICC 5.3 BC-OC	3.0*	64
Meinshausen et al., 2011	MAGICC 6.0	3.0*	53
Hartin et al., 2015 Hartin et al., 2016	Hector v2.0	3.0*	63
Millar et al., 2017	FAIR	2.7**	61
Myhre et al., 2013	AR5-IR	3.9**	62

*Unless otherwise noted.

** The ECS value for FAIR and AR5-IR is not adjustable (see S2)

Note: NA denotes models that have not reported an ESC value from Table 9.5 in IPCC AR5 (Flato et al., 2013).

S11 Simple Sensitivity Tests in SCMs

Here we discuss the SCM responses under a range of climate sensitivity and ocean diffusivity values.

S11.1 Changing Equilibrium Climate Sensitivity Values in SCMs with Comparison to CMIP5

We changed the ECS values in the SCMs to illustrate the effects of parameter selection on the model responses. We reproduce Figure 4 from the main paper using different ECS values in Hector v2.0, MAGCC 5.3, and MAGIC 6.0. We run each of these SCMs with a climate sensitivity values of 2.1°C, the same as GISS-E2-R, and 4.7°C, the same as MIROC-ESM. These two model values were selected because they represent the largest range of climate sensitivity values in the model data used here.

Figure S25 shows the global mean temperature response from 4xCO_2 concentration step in CMIP5 models and SCMs. The SCMs were run with two different ECS values. Figure S25a shows the SCM response with an ECS value of 2.1°C and Figure S25b shows the SCM responses with an ECS value of 4.7°C. We found that spanning the range of complex model ECS values still resulted in stronger SCM responses, which supports the conclusion in our main paper that the SCMs have a faster warming rate under strong forcing regimes compared to more complex models.

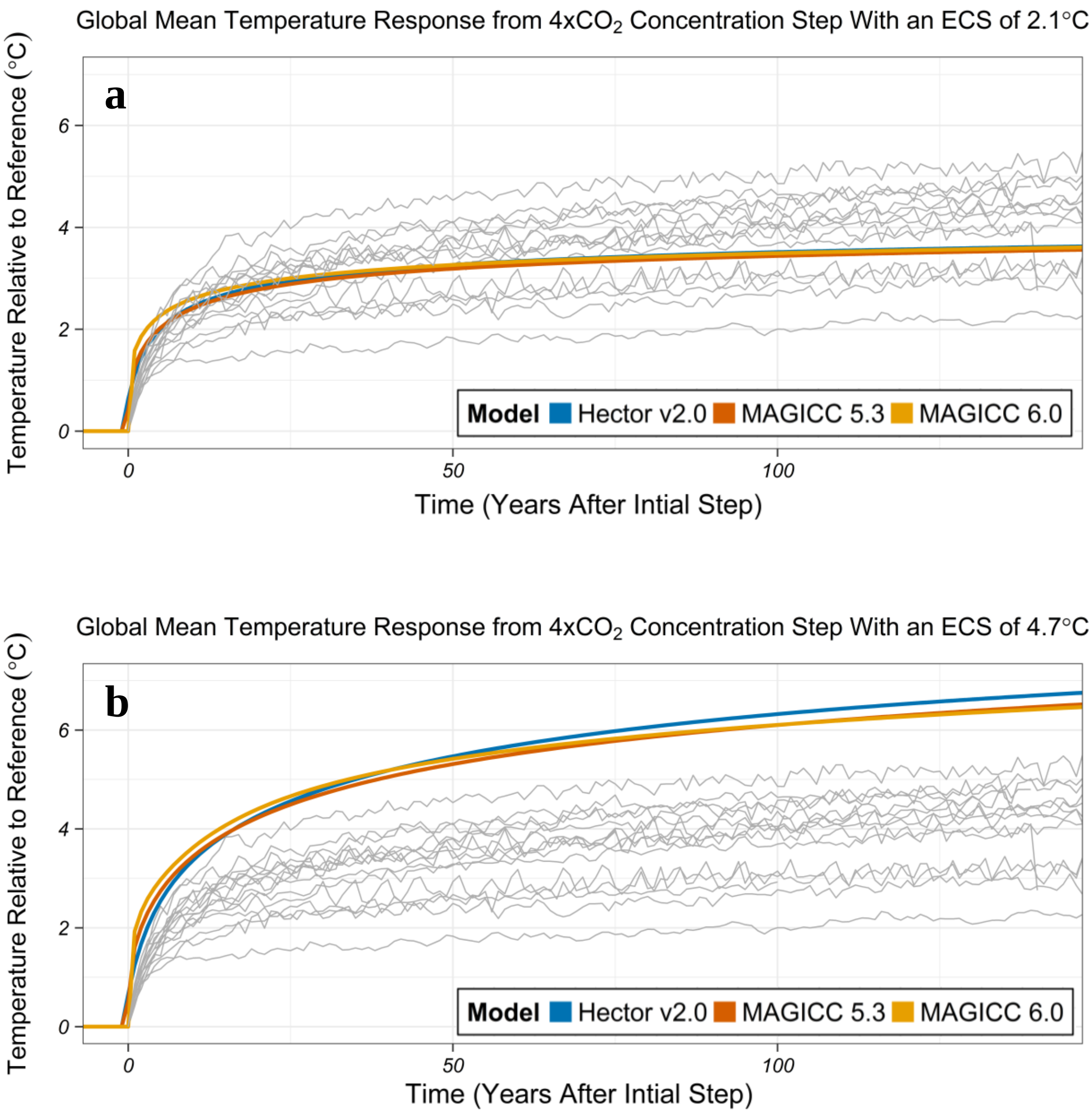

Figure S25 *Global mean temperature response from 4xCO2 concentration step in CMIP5 models and SCMs, as in Figure 5, with the SCMs run with two different ECS values. Figure 22a shows the SCM response with an ECS value of 2.1°C, and Figure 22b shows the SCM responses with an ECS value of 4.7°C (MAGICC 6.0 – yellow, MAGICC 5.3 BC-OC – red, Hector v2.0 – blue)*

S11.2 Additional Sensitivity Experiment in SCMs Using MAGICC6.0 Parameters

The aim of this paper is not to validate any individual SCM, nor the range of parameters used in the SCMs, which are also explored in the literature cited in our manuscript. Rather, we are evaluating the fundamental behavior of the simple models. However, understanding the uncertainty associated with our results is important.

In S11.1 we conducted a simple sensitivity test for the 4xCO_2 concentration step experiment by changing the climate sensitivity values in the three comprehensive SCMs used in this paper. Below, we have added some additional tests by exploring a range of climate sensitivity values and ocean diffusivity values in MAGICC 6.0 under a unit pulse of CO_2 emissions and a unit pulse of CO_2 concentration.

We selected climate sensitivity and ocean diffusivity values from the parameter ranges presented in Table 1B in Meinshausen et al. (2011). The values are the native MAGICC 6.0 parameters required to emulate complex models used in CMIP3 using three calibrated parameters (climate sensitivity, ocean diffusivity, and land/ocean warming). We provided the climate sensitivity and ocean diffusivity value ranges we explored in Table 11 below.

Table S11 MAGICC 6.0 parameter values from Meinshausen et al., 2011 Table 1B for sensitivity tests

Scenario	Climate sensitivity (K)	Ocean diffusivity (cm^2s^{-1})
Base Case	3.0	1.1
High Ocean diffusivity	3.0	3.74
Low Ocean diffusivity	3.0	0.50
High Climate sensitivity	6.03	1.1
Low Climate sensitivity	1.94	1.1

Figure S26 shows the global mean temperature response exploring the range of ocean diffusivity (Kz) (a) and global mean temperature response exploring the range of climate sensitivity (CS) (b) under a CO_2 emissions perturbation. Figure S27 shows the same results for under a CO_2 concentration pulse. Both figures illustrate that climate sensitivity has the greatest impact on the responses and in our manuscript, we accounted for this and used similar climate sensitivity values in SCMs where possible, unless otherwise noted in the supplemental figures.

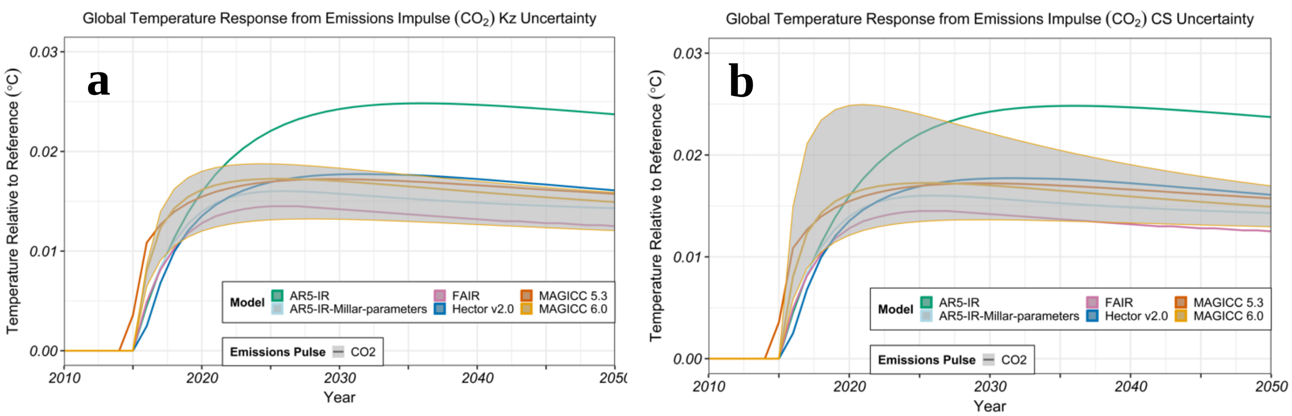

Figure S26 *Global mean temperature response exploring the range of ocean diffusivity (Kz) (a) and Global mean temperature response exploring the range of climate sensitivity (CS) (b) from a CO_2 emissions perturbation in SCMs. The grey shaded region in each figure shows the range in MAGICC 6.0 responses found using the Table S11 parameters. We note that the range of responses exploring CS (b) are normalized to account for the different climate conditions under difference CS values. (MAGICC 6.0 – yellow, MAGICC 5.3 BC-OC – red, Hector v2.0 – blue, AR5-IR – green, FAIR – pink, AR5-IR-Millar-parameters –light blue)*

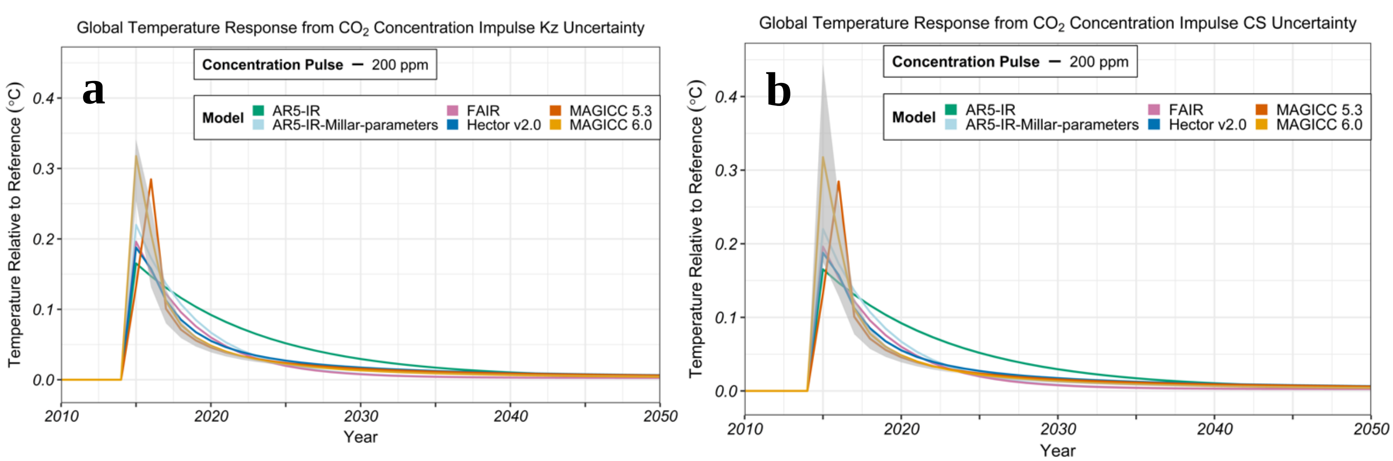

Figure S27 *Temperature response exploring the range of climate sensitivity (CS) (b) from a CO_2 concentration pulse in SCMs (MAGICC 6.0 – yellow, MAGICC 5.3 BC-OC – red, Hector v2.0 – blue, AR5-IR – green, FAIR –pink, AR5-IR-Millar-parameters –light blue). The grey shaded region in each figure shows the range in MAGICC 6.0 responses found using the Table R2 parameters. We note that the range of responses exploring CS (b) are normalized to account for the different climate conditions difference CS values.*

We acknowledge, however, that vertical ocean diffusivity has a large impact on ocean heat uptake and we do note that this parameter selection also impacts the responses in the SCMs, particular under a CO_2 emissions pulse (Meinshausen et al., 2011). However, the SCMs we compare in our paper either do not have the same definitions of vertical ocean diffusivity, as is the case for the comprehensive SCMs, or ocean diffusivity is not directly represented in the models, as is the case for idealized SCMs. For our purposes, therefore, we kept the ocean diffusivity values at their default values within the comprehensive SCMs.

For completeness, we also acknowledge that Meinshausen et al. (2011) spanned ranges of land/ocean warming contrast (RLO) in the three-parameter calibration described in Table 1B of their manuscript. And again, the SCMs either use the same values of RLO, as is the case for both versions of MAGICC, or this parameter is not represented in the idealized models. In fact, from our work using impulse response test to characterize SCMs, we concluded that SCMs without differential warming do not correctly capture the response pattern to BC perturbations.

S12 Comparison to Previous Impulse Responses Work by Joos et al. (2013)

We conducted the same perturbation experiment done by Joos et al. (2013) with our three comprehensive SCMs and two idealized SCMs, however, we do not conduct this against a constant CO_2 concentration background. Instead, we use the RCP 4.5 scenario and add a 100GtC CO_2 pulse in 2015. The versions used in each study differ slightly. Joos et al. used MAGICC model version 6.3 run in 171 different parameter settings that emulate 19 AOGCMs and 9 coupled climate-carbon cycle models. MAGICC 6.0 used in this study was set at the default setting using the AOGCM multi-model mean.

Table S12 shows the time-integrated airborne fraction at chosen time horizons from the 100 GtC pulse of CO_2 emissions. The Table S12 results are graphically represented in Figure S28. These results are largely discussed in the main paper.

Table S12 Time-integrated Airborne Fraction from a 100 GtC CO_2 Emissions Impulse in SCMs Compared to Results from Table 4 in Joos et al. (2013)

Time Horizon	**20 yr**	**50 yr**	**100 yr**
NCAR CSM1.4	13.8	27.8	46.6
HadGEM2-ES	14.7	30.9	53.3
MPI-ESM	14.5	29.2	48.8
Bern3D-LPJ (reference)	15.4	34.3	61.9
Bern3D-LPJ ensemble	15.1 (14.0-16.0)	32.7 (28.9-36.0)	57.6 (48.9-65.6)
Bern2.5D-LPJ	13.9	29.7	51.1
CLIMBER2-LPJ	13.0	26.8	49.2
DCESS	14.6	31.8	56.3
GENIE ensemble	13.6 (10.9-17.6)	28.9 (21.7-41.4)	50.5 (38.3-77.9)
LOVECLIM	13.5	27.9	45.3
MESMO	15.1	33.6	61.1
UVic2.9	13.7	29.5	53.0
ACC2	13.7	27.9	46.5
Bern-SAR	14.0	29.0	48.9
TOTEM2	16.9	38.3	66.6
MAGICC 6.0 ensemble	14.0 (12.0-16.1)	29.6 (23.6-35.7)	51.8 (40.0-64.2)
Multi-model mean	14.3 ± 1.8	30.2 ± 5.7	52.4 ± 11.3
Hector v2.0	16.2	34.0	58.3
MAGICC 5.3	16.0	33.4	58.3
MAGICC 6.0	15.3	32.2	57.9
AR5-IR	15.0	31.0	53.1
FAIR	14.6	32.6	61.6

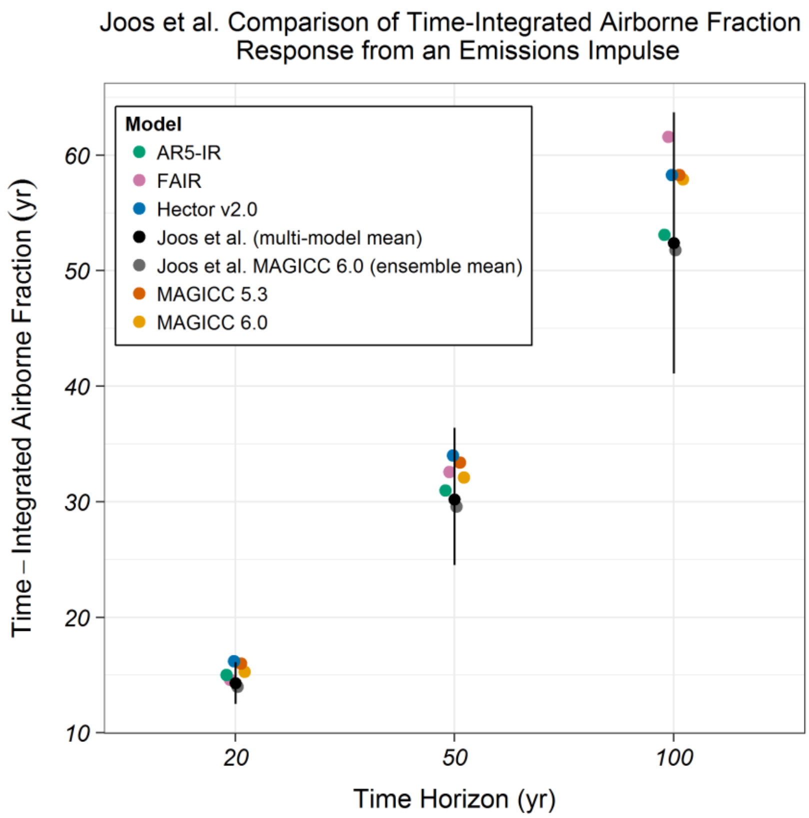

Figure S28 *Time-integrated airborne fraction from a 100GtC CO_2 emissions impulse in SCMs compared to Joos et al. This is not a direct comparison because we did not perform this experiment with a constant CO_2 concentration background, as done by Joos et al. The colored points represent the time-integrated airborne fraction in the SCMs used in this study, following Joos et al., and the Joos et al. MAGICC 6.0 ensemble mean. The black point is the Joos et al. multi-model mean and the vertical black line represents the range of the Joos et al. model results. (Joos et al. MAGICC 6.0 ensemble mean –grey, MAGICC 6.0 – yellow, MAGICC 5.3 BC-OC – red, Hector v2.0 – blue, AR5-IR – green, FAIR –pink).*

We also indirectly compare the temperature response of the comprehensive SCMs and more complex models in Joos et al. MAGICC 6.0 was used both here and by Joos et al., and we find similar responses with ≤ 1 °C yr difference from Joos et al. at each reported period. Though the other two comprehensive SCMs were not used by Joos et al., their similar responses to our MAGICC 6.0 allow us to make a larger conclusion, as done in the main paper. Using this logic, we are able to validate our SCM responses from a finite pulse. We find that the comprehensive SCM responses are generally less varied, close to the Joos et al. ensemble mean 20 years after the pulse, and below most Joos et al. model responses 50 and 100 years after the pulse (see Figure S29).

Table S13 Time-integrated temperature response from a 100 GtC CO_2 Emissions Impulse in SCMs Compared to Results from Table 7 in Joos et al. (2013).

Time Horizon	**20 yr**	**50 yr**	**100 yr**
NCAR CSM1.4	2.53	7.36	10.6
HadGEM2-ES	4.24	12.4	30.3
MPI-ESM	3.83	8.84	19.1
Bern3D-LPJ (reference)	4.11	12.1	24.5
Bern3D-LPJ ensemble	3.20 (2.1-4.6)	8.61 (5.1-13.5)	17.3 (9.5-29.3)
Bern2.5D-LPJ	3.15	8.40	17.1
CLIMBER2-LPJ	3.05	7.96	16.5
DCESS	3.38	9.96	20.6
GENIE ensemble	3.77	10.54	21.6
LOVECLIM	0.22	3.46	7.83
MESMO	4.41	12.5	26.0
UVic2.9	3.40	9.17	18.5
ACC2	3.99	10.55	20.0
Bern-SAR	n/a	n/a	n/a
TOTEM2	n/a	n/a	n/a
MAGICC 6.0 ensemble	3.64 (2.7-4.7)	8.96 (6.6-12.7)	17.2 (12-26)
Multi-model mean	3.29 ± 2.03	9.13 ± 4.45	18.7 ± 11.1
Hector v2.0	3.05	8.20	15.54
MAGICC 5.3	3.13	8.19	15.73
MAGICC 6.0	3.39	8.28	15.54

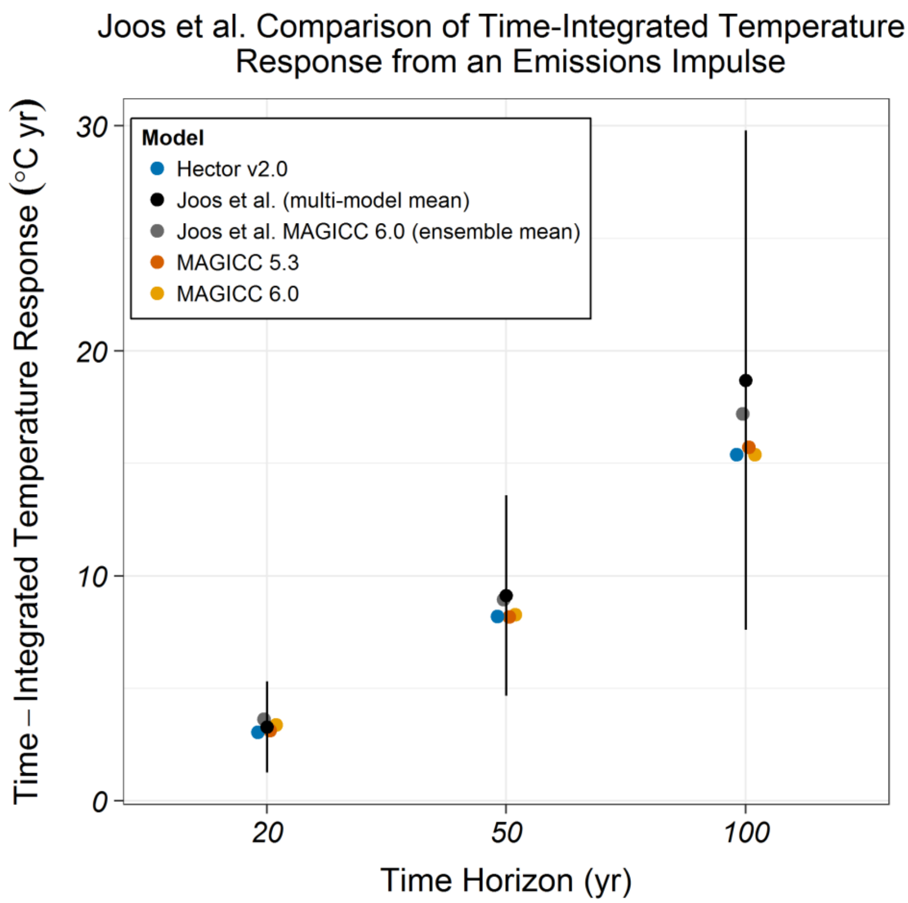

Figure S29 *Time-integrated temperature response from a 100GtC CO_2 emissions impulse in SCMs compared to Joos et al. This is not a direct comparison because we did not perform this experiment with a constant CO_2 concentration background, as done by Joos et al. The colored points represent the time-integrated temperature response in the SCMs used in this study, following Joos et al., and the Joos et al. MAGICC 6.0 ensemble mean. The black point is the Joos et al. multi-model mean and the vertical black line represents the range of the Joos et al. model results. (Joos et al. MAGICC 6.0 ensemble mean –grey, MAGICC 6.0 – yellow, MAGICC 5.3 BC-OC – red, Hector v2.0 – blue).*

We compare the comprehensive SCM responses from the 100GtC CO_2 pulse to our earlier experiment using a ~10GtC CO_2 pulse. We find that the relative behavior of the comprehensive SCMs in the 100 GtC CO_2 impulse is similar to the response pattern from the smaller pulse experiment (see Figure 3a and Figure S29). The MAGICC 6.0 temperature response pattern is consistent with our prior experiments, where we see an initially stronger response (10 years following the perturbation) compared to the other comprehensive SCMs. Due to the initial oscillatory behavior in complex model responses (see Figure 2a in Joos et al. (2013)), it is difficult to compare SCM responses to complex models on these short time scale.

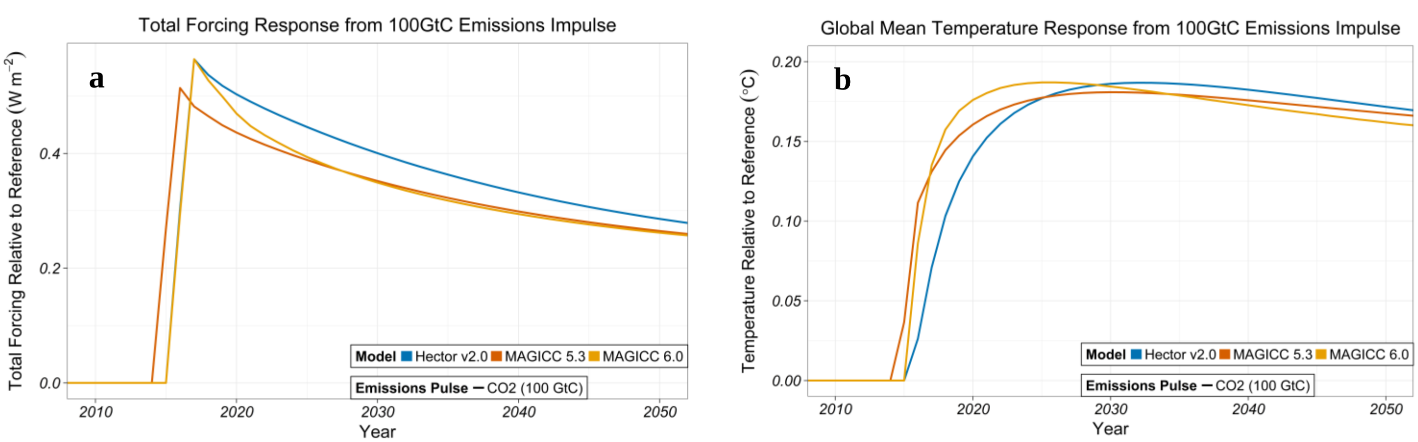

Figure S30 *Total forcing response (a) and global mean temperature response (b) from a 100GtC CO2 emissions impulse in the SCMs (MAGICC 6.0 – yellow, MAGICC 5.3 BC-OC – red, Hector v2.0 – blue).*

S13 Investigating Temperature Response from BC Step Experiment

We investigate SCM responses to a black carbon (BC) emissions step by quadrupling (4x) the values in 2015. We choose two of the SCMs, Hector v2.0 and MAGICC 5.3, as examples and compare the temperature response to Figure 1 in Sand et al. (2016). Sand et al. finds that after applying a 25x BC emissions step to NorESM1-M, a complex climate model, the temperature response levels off after less than 10 years. We find that temperature in both of these SCMs continue to increase over a century time-scale after the BC perturbation. The SCMs, therefore, fail to capture the temporal response to BC as seen in Sand et al. (2016), also seen in Yang et al. (2019).

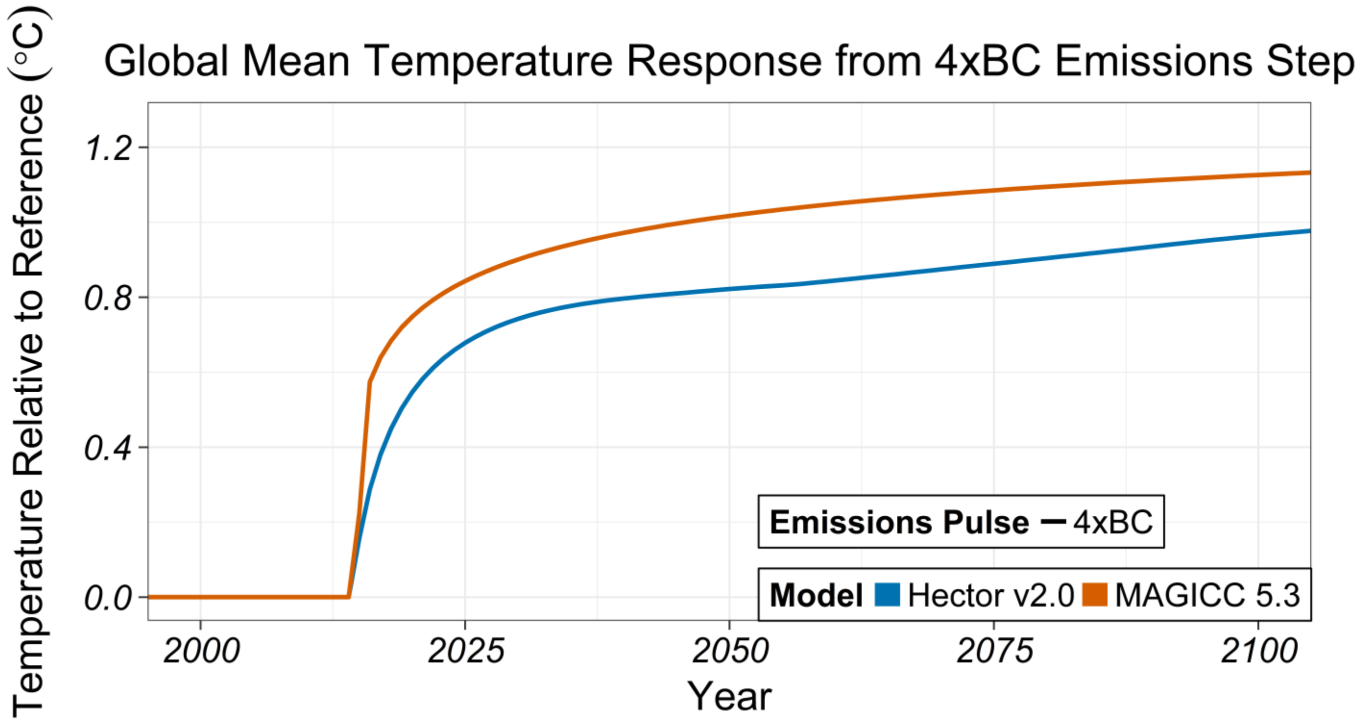

Figure S31 *Global mean temperature response from a 4xBC emissions step in the SCMs (MAGICC 5.3 BC-OC – red, Hector v2.0 – blue).*

S14 Supplementary Data

Other supplementary materials for this manuscript can be found at https://github.com/akschw04/Fundamental-Impulse-Tests-in-SCMs-Datasets and include the following:

Dataset S1 (separate file)

Simple climate model responses from 4xBC emissions step.

Dataset S2 (separate file)

Simple climate model responses from 4xCO_2 concentration step with 2.3 ocean diffusion and an ECS = 3 °C.

Dataset S3 (separate file)

Simple climate model responses from a 100PgC CO_2 emissions impulse experiment.

Dataset S4 (separate file)

Simple climate model responses from a CH_4 emissions impulse experiment.

Dataset S5 (separate file)

Simple climate model responses from a BC emissions impulse experiment.

Dataset S6 (separate file)

Simple climate model responses from CO_2 concentration impulse experiment.

Dataset S7 (separate file)

Simple climate model responses from CO_2 emissions impulse experiment.

Dataset S8 (separate file)

AR5-IR code to produce responses to BC emissions impulse.

Dataset S9 (separate file)

AR5-IR code to produce responses to CH_4 emissions impulse.

Dataset S10 (separate file)

AR5-IR code to produce responses to CO_2 emissions impulse.

Dataset S11 (separate file)

AR5-IR code to produce responses to 100PgC CO_2 emissions impulse for comparison to Joos *et al.* (2013)

Dataset S12 (separate file)

AR5-IR code to produce responses to CO_2 concentration step.

Dataset S13 (separate file)

FAIR CO_2 concentration impulse experiment input file.

Dataset S14 (separate file)

FAIR 4xCO_2 concentration step experiment input file.

Dataset S15 (separate file)

FAIR CO_2 emissions impulse experiment input file.

Dataset S16 (separate file)

FAIR 100Pg CO_2 emissions impulse experiment input file.

Dataset S17 (separate file)

FAIR CO_2 emissions impulse experiment reference input file.

Dataset S18 (separate file)

Hector v2.0 CO_2 concentration impulse experiment input file.

Dataset S19 (separate file)

Hector v2.0 CO_2 concentration impulse experiment reference input file.

Dataset S20 (separate file)

Hector v2.0 4xCO_2 concentration step experiment reference input file.

Dataset S21 (separate file)

Hector v2.0 4xCO_2 concentration step experiment input file.

Dataset S22 (separate file)

Hector v2.0 BC emissions impulse experiment input file.

Dataset S23 (separate file)

Hector v2.0 BC emissions step experiment input file.

Dataset S24 (separate file)

Hector v2.0 CH_4 emissions impulse experiment input file.

Dataset S25 (separate file)

Hector v2.0 CO_2 emissions impulse experiment input file.

Dataset S26 (separate file)

Hector v2.0 100Pg CO_2 emissions impulse experiment input file.

Dataset S27 (separate file)

Hector v2.0 emissions impulse experiment reference input file.

Dataset S28 (separate file)

Hector v2.0 emissions step experiment reference input file.

Dataset S29 (separate file)

MAGICC5.3 CO_2 concentration impulse experiment reference input file.

Dataset S30 (separate file)

MAGICC5.3 CO_2 concentration impulse experiment input file.

Dataset S31 (separate file)

MAGICC5.3 4xCO_2 concentration step experiment input file.

Dataset S32 (separate file)

MAGICC5.3 4xCO_2 concentration step experiment reference input file.

Dataset S33 (separate file)

MAGICC5.3 BC emissions impulse experiment input file.

Dataset S34 (separate file)

MAGICC5.3 BC emissions step experiment input file.

Dataset S35 (separate file)

MAGICC5.3 CH_4 emissions impulse experiment input file.

Dataset S36 (separate file)

MAGICC5.3 1% CO_2 emissions impulse experiment in 2010 input file.

Dataset S37 (separate file)

MAGICC5.3 1.01% CO_2 emissions impulse experiment in 2010 input file.

Dataset S38 (separate file)

MAGICC5.3 5% CO_2 emissions impulse experiment in 2010 input file.

Dataset S39 (separate file)

MAGICC5.3 10% CO_2 emissions impulse experiment in 2010 input file.

Dataset S40 (separate file)

MAGICC5.3 50% CO_2 emissions impulse experiment in 2010 input file.

Dataset S41 (separate file)

MAGICC5.3 100% CO_2 emissions impulse experiment in 2010 input file.

Dataset S42 (separate file)

MAGICC5.3 100% CO_2 emissions impulse experiment in 2015 input file.

Dataset S43 (separate file)

MAGICC5.3 100% CO_2 emissions impulse experiment in 2020 input file.

Dataset S44 (separate file)

MAGICC5.3 100% CO_2 emissions impulse experiment in 2030 input file.

Dataset S45 (separate file)

MAGICC5.3 100% CO_2 emissions impulse experiment in 2040 input file.

Dataset S46 (separate file)

MAGICC5.3 100% CO_2 emissions impulse experiment in 2050 input file.

Dataset S47 (separate file)

MAGICC5.3 100% CO_2 emissions impulse experiment in 2060 input file.

Dataset S48 (separate file)

MAGICC5.3 100% CO_2 emissions impulse experiment in 2070 input file.

Dataset S49 (separate file)

MAGICC5.3 100PgC CO_2 emissions impulse experiment in 2015 input file.

Dataset S50 (separate file)

MAGICC5.3 CO_2 emissions impulse experiment reference input file.

Dataset S51 (separate file)

MAGICC5.3 CO_2 emissions step experiment reference input file.

Dataset S52 (separate file)

MAGICC56.0 4xCO_2 concentration impulse experiment input file.

Dataset S53 (separate file)

MAGICC56.0 4xCO_2 concentration impulse experiment reference input file.

Dataset S54 (separate file)

MAGICC56.0 4xCO_2 concentration step experiment input file.

Dataset S55 (separate file)

MAGICC56.0 4xCO_2 concentration step experiment reference input file.

Dataset S56 (separate file)

MAGICC6.0 BC emissions impulse experiment input file.

Dataset S57 (separate file)

MAGICC6.0 CH_4 emissions impulse experiment input file.

Dataset S58 (separate file)

MAGICC6.0 100% CO_2 emissions impulse experiment input file.

Dataset S59 (separate file)

MAGICC6.0 100PgC CO_2 emissions impulse experiment input file.

Dataset S60 (separate file)

MAGICC6.0 emissions impulse experiment reference input file.

Dataset S61 (separate file)

MAGICC 6.0 MAGCFG_USER parameters.

Dataset S62 (separate file)

FAIRv1.0 model with general parameters.

Dataset S63 (separate file)

AR5-IR general parameters.

Dataset S64 (separate file)

Hector general parameters.

Dataset S65 (separate file)

MAGICC5.3 maggas_c parameters.

Dataset S66 (separate file)

MAGICC5.3 magice_c parameters.

Dataset S67 (separate file)

MAGICC5.3 magmod_c parameters.

Dataset S68 (separate file)

MAGICC5.3 magrun_c parameters.

Dataset S69 (separate file)

MAGICC5.3 maguser_c parameters.

Dataset S70 (separate file)

MAGICC5.3 magxtra_c parameters.

S15 References

Bakker, A. M. R., Wong, T. E., Ruckert, K. L. and Keller, K.: Sea-level projections representing the deeply uncertain contribution of the West Antarctic ice sheet, Sci. Rep., 7(1), 3880, doi:10.1038/s41598-017-04134-5, 2017.

Bond, T. C., Doherty, S. J., Fahey, D. W., Forster, P. M., Berntsen, T., Deangelo, B. J., Flanner, M. G., Ghan, S., Kärcher, B., Koch, D., Kinne, S., Kondo, Y., Quinn, P. K., Sarofim, M. C., Schultz, M. G., Schulz, M., Venkataraman, C., Zhang, H., Zhang, S., Bellouin, N., Guttikunda, S. K., Hopke, P. K., Jacobson, M. Z., Kaiser, J. W., Klimont, Z., Lohmann, U., Schwarz, J. P., Shindell, D., Storelvmo, T., Warren, S. G. and Zender, C. S.: Bounding the role of black carbon in the climate system: A scientific assessment, J. Geophys. Res. Atmos., 118(11), 5380–5552, doi:10.1002/jgrd.50171, 2013.

Cicerone, R.J.; Oremland, R. S.: GLOBAL BIOGEOCHEMICAL Methane (CH4) is the most abundant organic gas in measurement data has been reviewed by Ehhalt [1974] and Wofsy [1976] and will not be repeated here . Since the Earth ' s energy balance (see The quasi-steady state (defined in, , 2(4), 299–327, 1988.

Flato, G., Marotzke, J., Abiodun, B., Braconnot, P., Chou, S. C., Collins, W., Cox, P., Driouech, F., Emori, S., Eyring, V., Forest, C., Gleckler, P., Guilyardi, E., Jakob, C., Kattsov, V., Reason, C. and Rummukainen, M.: Evaluation of Climate Models, Clim. Chang. 2013 Phys. Sci. Basis. Contrib. Work. Gr. I to Fifth Assess. Rep. Intergov. Panel Clim. Chang., 741–866, doi:10.1017/CBO9781107415324, 2013.

Garner, G., Reed, P. and Keller, K.: Climate risk management requires explicit representation of societal trade-offs, Clim. Change, 134(4), 713–723, doi:10.1007/s10584-016-1607-3, 2016.

Geoffroy, O., Saint-martin, D., Olivié, D. J. L., Voldoire, A., Bellon, G. and Tytéca, S.: Transient climate response in a two-layer energy-balance model. Part I: Analytical solution and parameter calibration using CMIP5 AOGCM experiments, J. Clim., 26(6), 1841–1857, doi:10.1175/JCLI-D-12-00195.1, 2013.

Gupta, A. Sen, Jourdain, N. C., Brown, J. N. and Monselesan, D.: Climate drift in the CMIP5 models, J. Clim., 26(21), 8597–8615, doi:10.1175/JCLI_D_12_00521.1, 2013.

Harmsen, M. J. H. M., Van Vuuren, D. P., Van Den Berg, M., Hof, A. F., Hope, C., Krey, V., Lamarque, J.-F., Marcucci, A., Shindell, D. T. and Schaeffer, M.: How well do integrated assessment models represent non-CO 2 radiative forcing?, Clim. Change, 133, 565–582, doi:10.1007/s10584-015-1485-0, 2015.

Hartin, C. A., Patel, P., Schwarber, A., Link, R. P. and Bond-Lamberty, B. P.: A simple object-oriented and open-source model for scientific and policy analyses of the global climate system - Hector v1.0, Geosci. Model Dev., 8(4), 939–955, doi:10.5194/gmd-8-939-2015, 2015.

Hartin, C. A., Bond-Lamberty, B., Patel, P. and Mundra, A.: Ocean acidification over the next three centuries using a simple global climate carbon-cycle model: projections and sensitivities, Biogeosciences, 13, 4329–4342, doi:10.5194/bg-13-4329-2016, 2016.

Joos, F., Roth, R., Fuglestvedt, J. S., Peters, G. P., Enting, I. G., Von Bloh, W., Brovkin, V., Burke, E. J., Eby, M., Edwards, N. R., Friedrich, T., Frölicher, T. L., Halloran, P. R., Holden, P. B., Jones, C., Kleinen, T., Mackenzie, F. T., Matsumoto, K., Meinshausen, M., Plattner, G.-K. K., Reisinger, A., Segschneider, J., Shaffer, G., Steinacher, M., Strassmann, K., Tanaka, K., Timmermann, A. and Weaver, A. J.: Carbon dioxide and climate impulse response functions for the computation of greenhouse gas metrics: A multi-model analysis, Atmos. Chem. Phys., 13(5), 2793–2825, doi:10.5194/acp-13-2793-2013, 2013.

Kriegler, E.: Imprecise Probability Analysis for Integrated Assessment of Climate Change, Time, 258 [online] Available from: https://publishup.uni-potsdam.de/opus4-ubp/frontdoor/index/index/docId/497 (Accessed 29 October 2017), 2005.

Meinshausen, M., Raper, S. C. B. and Wigley, T. M. L.: Emulating coupled atmosphere-ocean and carbon cycle models with a simpler model, MAGICC6 - Part 1: Model description and calibration, Atmos. Chem. Phys., 11(4), 1417–1456, doi:10.5194/acp-11-1417-2011, 2011.

Millar, J. R., Nicholls, Z. R., Friedlingstein, P. and Allen, M. R.: A modified impulse-response representation of the global near-surface air temperature and atmospheric concentration response to carbon dioxide emissions, Atmos. Chem. Phys., 17(11), 7213–7228, doi:10.5194/acp-17-7213-2017, 2017.

Myhre, G., Shindell, D., Bréon, F.-M., Collins, W., Fuglestvedt, J., Huang, J., Koch, D., Lamarque, J.-F., Lee, D., Mendoza, B., Nakajima, T., Robock, A., Stephens, G., Takemura, T. and Zhang, H.: Anthropogenic and Natural Radiative Forcing, Clim. Chang. 2013 Phys. Sci. Basis. Contrib. Work. Gr. I to Fifth Assess. Rep. Intergov. Panel Clim. Chang., 659–740, doi:10.1017/ CBO9781107415324.018, 2013.

Raper, S. C. B. and Cubasch, U.: Emulation of the results from a coupled general circulation model using a simple climate model, Geophys. Res. Lett., 23(10), 1107–1110, doi:10.1029/96gl01065, 1996.

Sand, M., Berntsen, T. K., Von Salzen, K., Flanner, M. G., Langner, J. and Victor, D. G.: Response of Arctic temperature to changes in emissions of short-lived climate forcers, Nat. Clim. Chang., 6(3), 286–289, doi:10.1038/nclimate2880, 2016.

Smith, C. J., Forster, P. M., Allen, M., Leach, N., Millar, R. J., Passerello, G. A. and Regayre, L. A.: FAIR v1.3: A simple emissions-based impulse response and carbon cycle model, Geosci. Model Dev., 11(6), 2273–2297, doi:10.5194/gmd-11-2273-2018, 2018.

Smith, S. J. and Bond, T. C.: Two hundred fifty years of aerosols and climate: The end of the age of aerosols, Atmos. Chem. Phys., 14(2), 537–549, doi:10.5194/acp-14-537-2014, 2014.

Taylor, K. E., Stouffer, R. J. and Meehl, G. A.: An overview of CMIP5 and the experiment design, Bull. Am. Meteorol. Soc., 93(4), 485–498, doi:10.1175/BAMS-D-11-00094.1, 2012.

Thomson, A. M., Calvin, K. V., Smith, S. J., Kyle, G. P., Volke, A., Patel, P., Delgado-Arias, S., Bond-Lamberty, B., Wise, M. A., Clarke, L. E. and Edmonds, J. A.: RCP4.5: A pathway for stabilization of radiative forcing by 2100, Clim. Change, 109(1), 77–94, doi:10.1007/s10584-011-0151-4, 2011.

Urban, N. M., Holden, P. B., Edwards, N. R., Sriver, R. L. and Keller, K.: Historical and future learning about climate sensitivity, Geophys. Res. Lett., 41(7), 2543–2552, doi:10.1002/2014GL059484, 2014.

Wigley, T. M. L. and Raper, S. C. B.: Implications for climate and sea level of revised IPCC emissions scenarios, Nature, 357(6376), 293–300, doi:10.1038/357293a0, 1992.

Yang, Y., Smith, S. J., Wang, H., Mills, C. M. and Rasch, P. J.: Variability, timescales, and non-linearity in climate responses to black carbon emissions, Atmos. Chem. Phys. Discuss., 1–44, doi:10.5194/acp-2018-904, 2019.